Hypofunctional TrkA Accounts for the Absence of Pain Sensitization in the African Naked Mole-Rat

Graphical Abstract
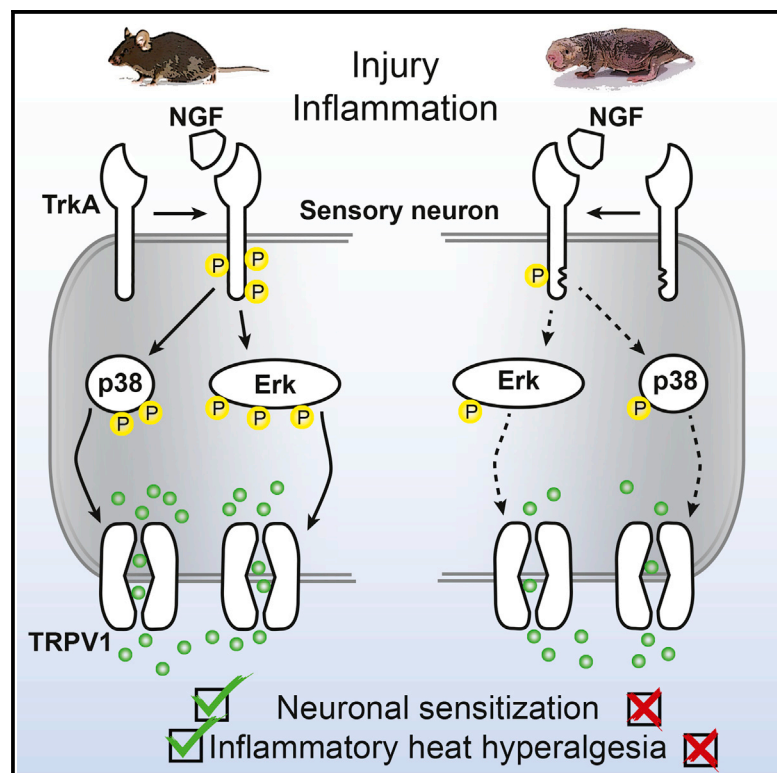
Authors

Damir Omerbašić, Ewan St. J. Smith, Mirko Moroni, ..., Chris G. Faulkes, Matthias Selbach, Gary R. Lewin

Correspondence

glewin@mdc-berlin.de

In Brief

Omerbašić et al. show that absent pain sensitization in naked mole-rats is associated with hypofunctional TrkA signaling. NGF stimulation of TrkA normally sensitizes TRPV1 channels, but not in naked mole-rat sensory neurons. The naked mole-rat TrkA kinase domain was shown to contain amino acid variants that attenuate TRPV1-dependent pain sensitization.

Highlights

- TRPV1 ion channels in naked mole-rat nociceptors are not sensitized by NGF

- Naked mole-rat TRPV1 channels are sensitized by NGF in mouse nociceptors

- NGF activation of naked mole-rat TrkA receptors does not sensitize TRPV1

- One to three amino acids in the naked mole-rat TrkA receptors may render it hypofunctional

CrossMark

CellPress

Hypofunctional TrkA Accounts for the Absence of Pain Sensitization in the African Naked Mole-Rat

Damir Omerbašić,[1,5,7] Ewan St. J. Smith,[1,2,7] Mirko Moroni,[1] Johanna Homfeld,[1] Ole Eigenbrod,[1] Nigel C. Bennett,[3] Jane Reznick,[1] Chris G. Faulkes,[4] Matthias Selbach,[5] and Gary R. Lewin[1,6,8,*]

[1]Molecular Physiology of Somatic Sensation, Max Delbrück Center for Molecular Medicine, 13125 Berlin, Germany
[2]Department of Pharmacology, University of Cambridge, Cambridge CB2 1PD, UK
[3]Department of Zoology and Entomology, University of Pretoria, Pretoria, Hatfield 0028, Republic of South Africa
[4]School of Biological and Chemical Sciences, Queen Mary University of London, Mile End Road, London E1 4NS, UK
[5]Proteome Dynamics Group, Max Delbrück Center for Molecular Medicine, 13125 Berlin, Germany
[6]Excellence Cluster Neurocure, Charité Universitätsmedizin Berlin, 10117 Berlin, Germany
[7]Co-first author
[8]Lead Contact
*Correspondence: glewin@mdc-berlin.de
http://dx.doi.org/10.1016/j.celrep.2016.09.035

SUMMARY

The naked mole-rat is a subterranean rodent lacking several pain behaviors found in humans, rats, and mice. For example, nerve growth factor (NGF), an important mediator of pain sensitization, fails to produce thermal hyperalgesia in naked mole-rats. The sensitization of capsaicin-sensitive TRPV1 ion channels is necessary for NGF-induced hyperalgesia, but naked mole-rats have fully functional TRPV1 channels. We show that exposing isolated naked mole-rat nociceptors to NGF does not sensitize TRPV1. However, the naked mole-rat NGF receptor TrkA displays a reduced ability to engage signal transduction pathways that sensitize TRPV1. Between one- and three-amino-acid substitutions in the kinase domain of the naked mole-rat TrkA are sufficient to render the receptor hypofunctional, and this is associated with the absence of heat hyperalgesia. Our data suggest that evolution has selected for a TrkA variant that abolishes a robust nociceptive behavior in this species but is still compatible with species fitness.

INTRODUCTION

Inflammation and tissue injury cause hypersensitivity of the affected tissue so that mild mechanical and thermal stimuli become painful. This phenomenon is called hyperalgesia (Lewin et al., 2014; Smith and Lewin, 2009). A critical endogenous mediator of inflammatory thermal and mechanical hyperalgesia, both in rodents and in humans, is nerve growth factor (NGF). Early studies in rodents and humans revealed that a single local dose of exogenous recombinant NGF can produce profound and long-lasting thermal and mechanical hyperalgesia (Dyck et al., 1997; Lewin and Mendell, 1993; Lewin et al., 1993; Petty et al., 1994). Furthermore, loss of function mutations in the *NGF* gene or *NTRK1*, which encodes the high-affinity NGF re-

ceptor TrkA, cause a range of congenital pain insensitivity syndromes in humans (Carvalho et al., 2011; Einarsdottir et al., 2004; Indo et al., 1996). The NGF/TrkA signaling system is critical for the genesis and maintenance of hypersensitivity states in mammals (Lewin et al., 1994, 2014; Woolf et al., 1994). The importance of increased NGF signaling during pain has recently been reinforced by the fact that blocking NGF signaling appears to be highly effective in treating pain in humans on the basis of phase 2 clinical trial data (Katz et al., 2011; Lane et al., 2010).

The naked mole-rat (*Heterocephalus glaber*) is a eusocial African rodent that displays a range of extreme physiological characteristics from cancer resistance and extreme longevity to complete insensitivity to acid (Liang et al., 2010; O'Connor et al., 2002; Park et al., 2008; Smith et al., 2011; Schuhmacher et al., 2015). We discovered that this species completely lacks behavioral heat hyperalgesia when challenged with NGF and the pro-inflammatory agents capsaicin and complete Freund's adjuvant (Park et al., 2008). The polymodal, capsaicin-gated ion channel TRPV1 is also required in mice for the development of NGF-induced heat hyperalgesia (Chuang et al., 2001). However, our studies have shown that although naked mole-rats are behaviorally insensitive to capsaicin, they have sensory neurons that express a TRPV1 channel with ligand sensitivity and biophysical properties indistinguishable from that found in mice or humans (Smith et al., 2011). Here, we investigated how heat hyperalgesia has been disabled in the naked mole-rat over the course of evolution. We addressed this question using molecular and cellular approaches to dissect out at which stage of the sensitization pathway heat sensitization fails. A cellular model of heat hyperalgesia is the rapid and potent sensitization of TRPV1 currents that has been studied in isolated sensory neurons (Shu and Mendell, 2001). We show that rapid sensitization of TRPV1-mediated currents is absent in sensory neurons from naked mole-rats. However, the naked mole-rat TRPV1 protein can be sensitized when expressed in mouse sensory neurons. We show that the cloned naked mole-rat TrkA receptor is less efficient at engaging signal transduction pathways leading to TRPV1 sensitization. Furthermore, we demonstrate that unique amino acid variants in the kinase domain of the naked mole-rat
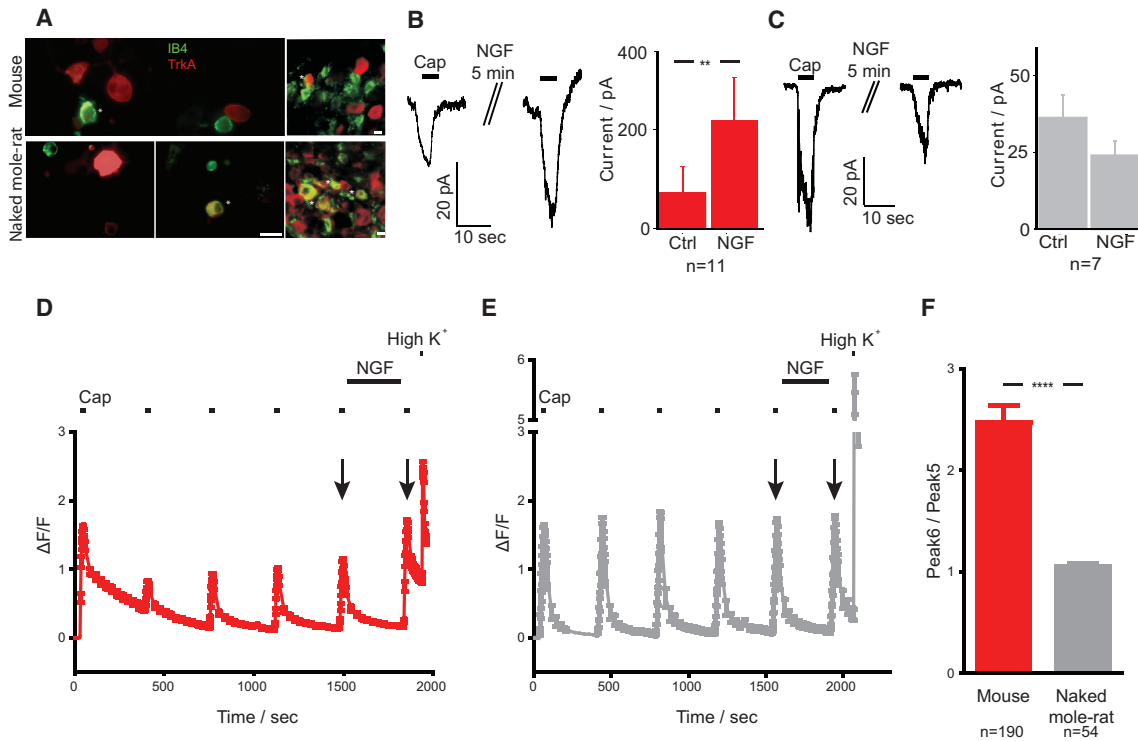
Figure 1. Naked Mole-Rat Dorsal Root Ganglia Neurons Are Not Sensitized by NGF

(A) IB4 (green) and TrkA (red) label largely different populations of mouse DRG neurons, greater co-labeling occurs in naked mole-rat TrkA-positive DRG neurons in culture (left panels) and sections (right panels). Asterisks denote double-labeled neurons; scale bar, 20 μm.

(B and C) NGF potentiates capsaicin-gated currents in mouse DRG neurons (B) but has no effect in naked mole-rat neurons (C).

(D and E) NGF superfusion causes sensitization of mouse DRG neurons, observed as increase in calcium influx (D), but not in naked mole-rat DRG neurons (E); high-potassium solution (40 mM KCl) was used to verify cell viability.

(F) Ratios of sixth and fifth capsaicin response from (D) and (E), as labeled by arrows.

Mann-Whitney *U* test was used in (B), (C), and (F) (**p < 0.01; ****p < 0.0001). Data are presented as mean ± SEM.

TrkA receptor likely render the receptor hypofunctional. Thus, millions of years of evolution appear to have led to an efficient and possibly single-molecule change that disables heat hyperalgesia.

RESULTS

TRPV1 Is Not Sensitized by NGF in Naked Mole-Rat Nociceptors

We made whole-cell patch-clamp recordings from isolated mouse and naked mole-rat sensory neurons live-labeled with fluorescently tagged isolectin B4 (IB4). IB4 predominantly binds to non-peptidergic small-diameter sensory neurons in mice, while TrkA immunoreactivity is specific to peptidergic sensory neurons that do not bind IB4 (Averill et al., 1995). Immunohistochemistry confirmed that IB4-negative sensory neurons are TrkA positive in mouse and naked mole-rat, but as in the rat (Price and Flores, 2007), some naked mole-rat TrkA-positive neurons were IB4 positive (Figure 1A). We also immunostained cultured naked mole-rat sensory neurons and found that 50% (34/68 cells) were TrkA positive while 35% (24/68) were IB4 positive, and only a small proportion of TrkA-positive cells were IB4 positive (15% [5/34]). We thus focused our analysis on IB4-negative neu-

rons to increase the likelihood of recording from naked mole-rat sensory neurons that possess TrkA receptors. The ability of NGF to rapidly sensitize TRPV1 was measured by comparing capsaicin-evoked current amplitudes before and after a 5-min NGF superfusion (100 ng/mL). As in rat sensory neurons (Shu and Mendell, 1999), there was a substantial increase in the average size of the capsaicin-evoked current (>2-fold) after acute NGF treatment of IB4-negative mouse sensory neurons (Figure 1B). However, in naked mole-rat IB4-negative sensory neurons, NGF never sensitized TRPV1 currents (Figure 1C). In order to confirm these results we also performed calcium imaging on isolated mouse and naked mole-rat sensory neurons. Given that both capsaicin and calcium influx cause desensitization and tachyphylaxis of TRPV1 (Koplas et al., 1997; Lishko et al., 2007), we applied five consecutive pulses (100 nM capsaicin, 30 s pulse) in order to obtain stable calcium signals before exposing the neurons to NGF (Hanack et al., 2015), followed by the sixth capsaicin pulse (Figures 1D and 1E). In mouse sensory neurons, NGF caused robust sensitization of capsaicin responses, but no increase in calcium influx was observed in naked mole-rat sensory neurons (Figure 1F). Thus, the absence of behavioral signs of NGF-induced heat hyperalgesia in the naked mole-rat (Park et al., 2008) can be accounted for by molecular changes, intrinsic
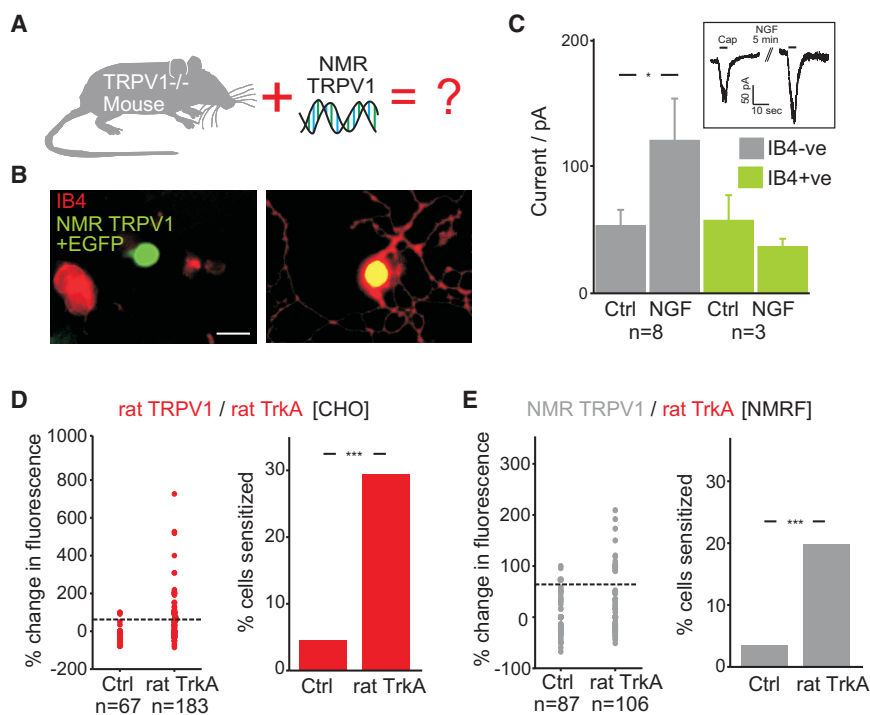
Figure 2. Naked Mole-Rat TRPV1 Currents Can Be Sensitized by NGF

(A) Naked mole-rat *Trpv1* cDNA was transfected into DRG neurons originating from *Trpv1*$^{-/-}$ mice.

(B) *Trpv1*$^{-/-}$ DRG neurons expressing naked mole-rat TRPV1 channels were identified by co-transfection with *EGFP*; IB4-568 labeling allowed targeting of TrkA-positive neurons. Scale bar, 50 μm.

(C) NGF potentiates naked mole-rat TRPV1-mediated capsaicin currents in IB4-negative, but not IB4-positive, *Trpv1*$^{-/-}$ DRG neurons.

(D) In CHO cells co-expressing rat *Trpv1*/rat *TrkA*, NGF sensitized capsaicin responses, unlike in control cells.

(E) Naked mole-rat fibroblast cells expressing naked mole-rat *Trpv1*/rat*TrkA* were sensitized by NGF when compared to controls.

Sensitization in (D) and (E) was scored if change in [Ca^{2+}]$_i$ intensity > (mean + 2 SD) of controls (dotted lines in lefthand panels). Mann-Whitney *U* test was used in (C) and chi-square test in (D) and (E) (*p < 0.05; ***p < 0.001). Data in (C) are presented as mean ± SEM.

to naked mole-rat nociceptors, that have disabled NGF sensitization of TRPV1.

The cloned naked mole-rat *TRPV1* receptor (*nmrTrpv1*) displays biophysical properties similar to its mouse counterpart with respect to proton, capsaicin, and heat gating (Smith et al., 2011). It is, however, possible that the naked mole-rat TRPV1 protein cannot be phosphorylated on critical residues that are required for full sensitization. Several conserved amino acid residues that can be phosphorylated within the TRPV1 molecule have been shown to be important for sensitization (Bhave et al., 2003; Chuang et al., 2001; Prescott and Julius, 2003; Zhang et al., 2005); however, all but one of these residues were conserved in *nmrTrpv1* (Figure S1A). Thus, Ser502 (numbering for *ratTrpv1*), a normally conserved residue involved in protein kinase C epsilon type (PKCε)-mediated sensitization (Numazaki et al., 2002), was substituted by a threonine in the naked mole-rat protein. By using the phorbol-12-myristate-13-acetate ester (PMA) to activate PKCε in cells transfected with *ratTrpv1*, we observed robust sensitization using calcium imaging as the readout (Figure S1B). To measure PKCε sensitization of *nmrTRPV1*, we used a new naked mole-rat fibroblast cell line (Figure S1C) to enable recording of PKCε-mediated sensitization of *nmrTRPV1* in its native environment, which was robustly observed (Figure S1D). We also generated a naked mole-rat TRPV1^{T502S} mutant that was also sensitized by PMA in naked mole-rat fibroblast cell lines (Figure S1E) and conclude that in terms of TRPV1 sensitization, threonine is functionally equivalent to serine at position 502.

To demonstrate more directly that naked mole-rat TRPV1 is fully capable of being sensitized, we expressed it in mouse sensory neurons from *Trpv1*$^{-/-}$ mice. Using an Alexa-Fluor-568-

conjugated IB4, mouse *Trpv1*$^{-/-}$ IB4-negative sensory neurons were selected by their green fluorescence after transfection with plasmids encoding EGFP and the naked mole-rat *Trpv1* cDNA (Figures 2A and 2B). We used whole-cell patch-clamp electrophysiology to demonstrate that capsaicin-evoked currents are present in transfected *Trpv1*$^{-/-}$ sensory neurons and that these currents could be sensitized by NGF (Figure 2C). In contrast, no sensitization of the capsaicin current in mouse IB4-positive sensory neurons was observed presumably because of the absence of TrkA in these cells (Figures 2C and 1A). Transfected *Trpv1*$^{-/-}$ sensory neurons had heat-gated currents with an activation threshold of 44.4°C ± 0.7°C (n = 5) and pH-gated currents sensitive to ruthenium red (Figure S1F). Heat-activated currents are reported to be otherwise rare in *Trpv1*$^{-/-}$ sensory neurons (Caterina et al., 2000). Thus, the naked mole-rat TRPV1 protein can rescue capsaicin and heat sensitivity in *Trpv1*$^{-/-}$ sensory neurons with a heat-activation threshold concomitant with the heat-activation threshold of nmrTRPV1 (Smith et al., 2011) and is fully capable of NGF initiated sensitization in the mouse cellular context.

Rapid TRPV1 sensitization via NGF activation of TrkA receptors can be reconstituted in human and animal-derived cell lines as well as *Xenopus laevis* oocytes (Bonnington and McNaughton, 2003; Prescott and Julius, 2003; Zhang et al., 2005). It is possible that TRPV1 sensitization by NGF cannot take place in the naked mole-rat cellular context. We used calcium imaging to measure TRPV1 sensitization after Chinese hamster ovary (CHO) cells were transfected with *ratTrpv1*/*ratTrkA*. In control experiments, *ratTrkA* was either not transfected or buffer instead of NGF was superfused between the capsaicin pulses. NGF produced a robust sensitization with 29.5% of capsaicin-responsive CHO cells showing increased calcium signals post-NGF compared to just 4.5% in controls (Figure 2D). Similarly, using naked mole-rat fibroblast cells

co-transfected with *nmrTrpv1/ratTrkA*, 19.8% of capsaicin-responsive naked mole-rat fibroblast cells showed increased calcium signals post-NGF compared to just 3.5% in controls (Figure 2E). These data indicate that naked mole-rat cells possess the necessary signaling components for TRPV1 sensitization.

Naked Mole-Rat TrkA Is Hypofunctional

We cloned the naked mole-rat *TrkA* cDNA from mRNA isolated from sensory neurons (*nmrTrkA*). The *nmrTrkA* sequence was identical to that predicted from the naked mole-rat genome assembly (Keane et al., 2014; Kim et al., 2011). The predicted naked mole-rat TrkA peptide sequence was aligned with orthologous sequences from 26 other mammalian species (Figure S2). There was significant sequence divergence in the extracellular TrkA domains, including the juxtamembrane NGF-binding domain; however, the intracellular sequences within the kinase domain were highly conserved (Figure S2B). All tyrosine residues important for receptor activation were conserved in all the species, including the naked mole-rat. We reasoned that at least some of the amino acid variants in the kinase domain of *nmrTrkA* may be common variants found in African mole-rats (family Bathyergidae). In order to screen for such variants, we obtained TrkA sequences from five further African mole-rat species: the Damaraland mole-rat (*Fukomys damarensis*), the Mashona mole-rat (*Fukomys darlingi*), the giant mole-rat (*Fukomys mechowii*), the Natal mole-rat (*Cryptomys hottentotus natalensis*), and Emin's mole-rat (*Heliophobius emini*) (Figure S3A). We used genomic DNA from these species to PCR amplify the exonic regions of the TrkA gene, guided by variants found in nmrTrkA. However, we also assembled TrkA transcripts from published RNA sequencing (RNA-seq) data from African mole-rat species (Davies et al., 2015). In addition, we obtained RNA from the brains of three Mashona mole-rats and performed RNA-seq followed by de novo transcriptome assembly (Table S1). An African mole-rat phylogeny was constructed including the new transcriptome data from the Mashona mole-rat (Figure S3C), and this was in close agreement with previous analyses that had not included this species (Davies et al., 2015). Alignment of the available predicted TrkA amino acid sequences from African mole-rats revealed that the nmrTrkA kinase domain has accumulated at least three amino acid variants that are either absent or rare in the animal kingdom, including African mole-rats (Figure S3B). There was just one amino acid change that appeared to be unique to naked mole-rat, which was a leucine (rat) to cysteine substitution at position 774 (Figure S2B). The accumulation of amino acid variants in the *nmrTrkA* kinase domain encouraged us to carry out a functional analysis of the ability of this receptor to participate in nociceptor sensitization. To do this, we tested the ability of the naked mole-rat TrkA receptor to sensitize TRPV1 using electrophysiology with *X. laevis* oocytes as the heterologous expression system. Oocytes were injected with a *ratTrpv1* cRNA and cRNAs coding for either *ratTrkA* or *nmrTrkA*. We observed that 1 μM capsaicin causes substantial and long-lasting desensitization of TRPV1 currents in oocytes and thus decided to record proton-gated TRPV1 currents to quantify NGF sensitization, as others have done (Zhang et al., 2005). Using a two-electrode voltage clamp, we showed that

an acidic stimulus (pH 5.8) produced robust inward currents in TRPV1-expressing oocytes that were absent in non-injected oocytes (data not shown). In oocytes injected with *ratTrkA* and *ratTrpv1* cRNA, superfusion of NGF (100 ng/mL, 5 min) caused a robust sensitization of acid-gated currents (Figure 3B). However, the same NGF concentration produced a significantly smaller sensitization of TRPV1 currents in oocytes injected with *nmrTrkA* and *ratTrpv1* cRNA (Figures 3B and 3E). Comparable amounts of rat and naked mole-rat TrkA protein were present in membranes isolated from *X. laevis* oocytes (Figure 3C), indicating that differences in TrkA protein levels was unlikely to account for the reduced TRPV1 sensitization. We next varied NGF concentration (1–1,000 ng/mL) but kept the superfusion time constant (5 min). TrkA is a high-affinity NGF receptor with a dissociation constant K_d of less than 10^{-9} M (Kaplan et al., 1991; Klein et al., 1991). When oocytes were stimulated with 1,000 ng/mL NGF, activation of the naked mole-rat TrkA receptor produced a degree of sensitization similar to that observed with rat TrkA (Figure 3C). These results strongly suggest that the naked mole-rat TrkA molecule is less efficient at initiating sensitization with NGF concentrations of ∼100 ng/mL, which was shown to be saturating in adult rat sensory neurons (Shu and Mendell, 1999). It is conceivable that recombinant human NGF used in this study (rhNGF) displays stronger binding affinity to rat TrkA than to the naked-mole-rat TrkA. To test this idea, we cloned chimeric TrkA receptors containing the N-terminal, extracellular part of the receptor from rat TrkA together with the transmembrane domain and entire intracellular kinase domain from the naked mole-rat molecule (Figures 3D and 3E). HEK293 cells were transiently transfected with either rat or chimeric *TrkA* construct to assess NGF-stimulated TrkA activation (Figure S4). An antibody raised against extracellular rat TrkA domain was used to measure the total level of TrkA protein in cell lysates (total TrkA), and two antibodies that recognize phosphorylated tyrosine residues in the TrkA kinase domain were employed to study receptor activation. Anti-phospho-TrkA (Tyr674/675; numbering for human TrkA) was used to measure the phosphorylation levels of the activation loop tyrosines (Segal and Greenberg, 1996; Segal et al., 1996), and an anti-phospho-TrkA (Tyr490) was used that recognizes the activated putative Shc binding site (Obermeier et al., 1993a). NGF stimulation triggered rapid phosphorylation of Tyr674/675 in rat TrkA, but not in chimeric TrkA (Figures S4A and S4B). In contrast to rat TrkA, NGF treatment did not have any effect on activation of Tyr674/675 in the chimeric TrkA receptor. However, the Tyr674/675 residues in both chimeric TrkA and rat TrkA displayed strong basal receptor phosphorylation in the absence of NGF, probably triggered by receptor dimerization events due to overexpression. This observation is in agreement with previous findings that an antibody against the TrkA extracellular domain can itself crosslink two receptors, causing their activation in PC12 cells (Clary et al., 1994; Hempstead et al., 1992). NGF triggered increased phosphorylation of the Tyr490 residue in the rat TrkA molecule after 1 min but did not have any apparent effect on the phosphorylation level of the chimeric TrkA Tyr490 residue (Figures S4C and S4D). Next, we tested chimeric TrkA in the context of NGF-mediated TRPV1 sensitization. Proton acid-gated TRPV1 currents in *X. laevis* oocytes co-expressing chimeric TrkA could only be
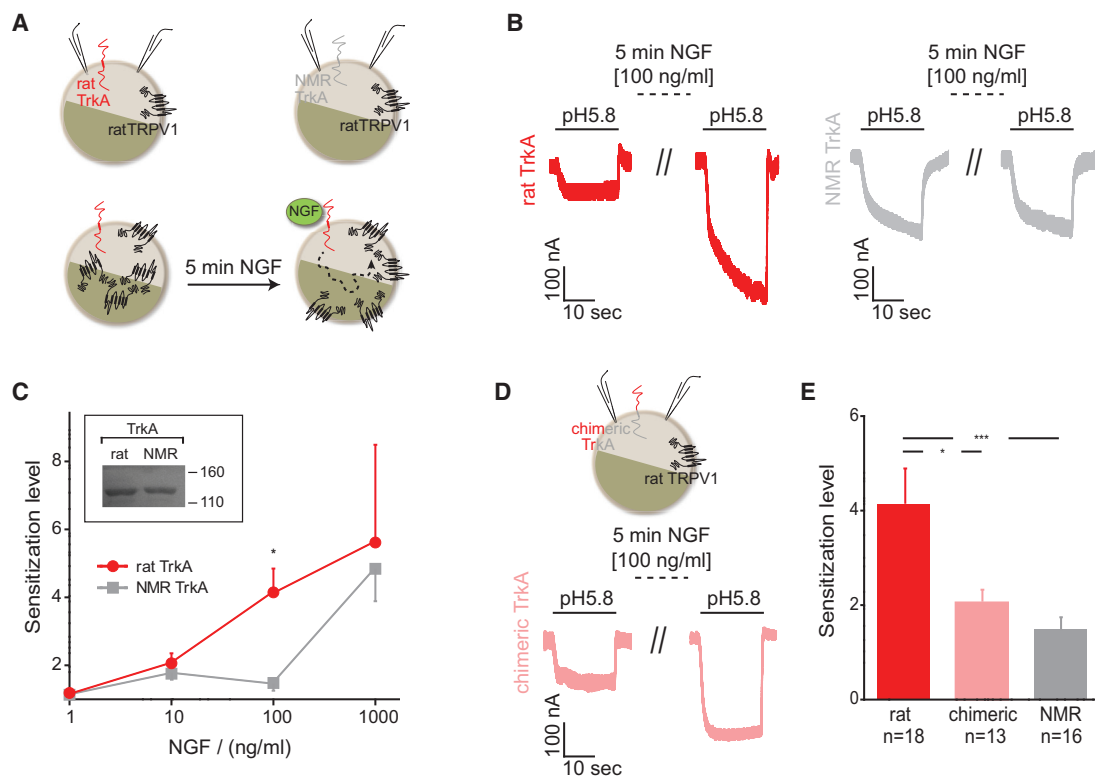
Figure 3. Naked Mole-Rat TrkA Is Impaired in TRPV1 Current Potentiation

(A) Schematic representation of the transfection and recording conditions used.

(B) NGF causes substantial sensitization of proton-gated rat TRPV1 currents when signaling through rat TrkA, but this effect is reduced in the oocytes co-expressing the naked mole-rat TrkA receptor.

(C) Sensitization levels across NGF concentrations were calculated as the ratio of a current immediately after and before NGF superfusion. High NGF concentration rescues the sensitization through NGF TrkA. For all the measurements, at least three pH stimuli were applied before the NGF superfusion in order to obtain the stable current responses, while at least two acid-gated currents were recorded post-NGF application. Between 2 and 18 oocytes were recorded for every NGF concentration. Inset: ten oocytes, injected with equal concentration of rat or naked mole-rat*TrkA* cRNA, were lysed, and pelleted membranes were subjected to western blotting. Prior to blotting, the protein concentration was measured to ensure equal sample loading. TrkA is expressed as a 140-kDa protein.

(D and E) 100 ng/mL NGF potentiated acid-gated TRPV1 currents recorded in *X. laevis* oocytes via chimeric TrkA (D), but the sensitization level was significantly smaller than for rat TrkA and not different from the NMR TrkA receptor quantified in (E).

Two-way ANOVA with Sidak's multiple comparison was used in (C), and one-way ANOVA with Bonferroni's multiple comparison test was used in (E) (*p < 0.05; ***p < 0.001). Data are presented as mean ± SEM, except in (C) for NMR TrkA at 1 ng/mL NGF (only mean current plotted), where two oocytes were recorded.

moderately sensitized with 100 ng/mL NGF; indeed, the mean level of sensitization observed was not significantly larger than that found with the full-length *nmrTrkA* (Figure 3E). In contrast, sensitization of TRPV1 proton currents by NGF-stimulated oocytes co-expressing *ratTrkA* was at least twice as large as with full-length *nmrTrkA* or chimeric receptors. These results strongly suggest that a hypo-functional naked mole-rat TrkA kinase domain underlies the lack of TRPV1 sensitization in this species.

Quantitative Proteomics Reveals Hypofunctional Downstream Signaling of the nmrTrkA Intracellular Domain

A quantitative proteomics approach was used that combined HEK293 cell stable isotope labeling by amino acids in cell culture (SILAC) (Ong et al., 2002) with high-resolution liquid chromatography coupled with tandem mass spectrometry (LC-MS/MS). Heavy-stable isotope (Lys-8 and Arg-10)-labeled HEK cells tran-

siently expressing rat or chimeric TrkA were stimulated with murine NGF (100 ng/mL) for 10 min and light-stable isotope (Lys-0 and Arg-0) cells were left untreated (Figure 4A) (Olsen et al., 2006). Following stimulation, cells were lysed, and equal amounts of protein were used for each SILAC pair (Figure 4A). Titanium dioxide (TiO_2) chromatography was used for phosphopeptide enrichment, and peptides were analyzed with LC-MS/MS. Typically, phosphopeptides were sequenced several times in different forms (such as oxidized methionine or missed tryptic cleavage), and overall, a similar number of phosphopeptide sites were quantified and identified in cells transfected with rat TrkA or chimeric TrkA (Figure 4B), indicating a similar overall number of phosphorylated proteins in each condition. Class I phosphopeptide sites comprise those residues with the highest localization probability for the phospho-group (>0.75); that is, the sum of probabilities of other potential sites is less than 0.25. From more than 2,000 identified and quantified class I phospho-sites,
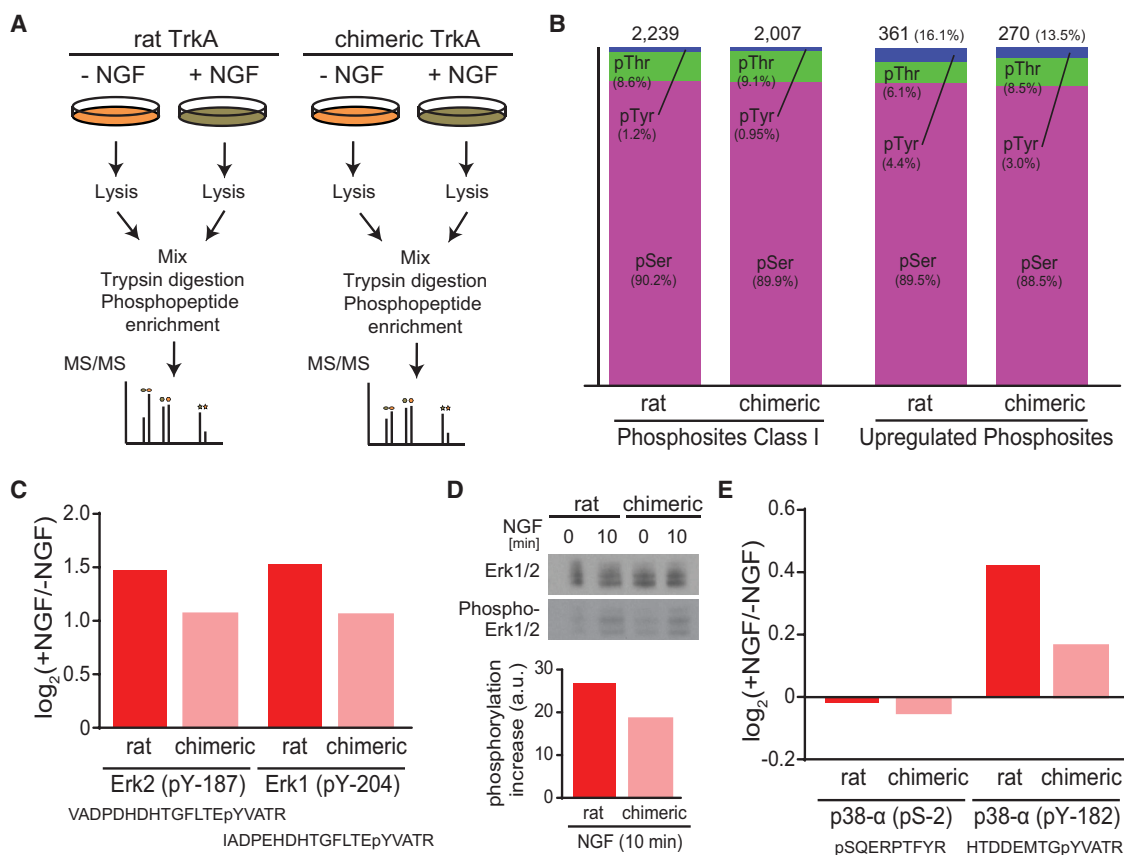
Figure 4. Quantitative Proteomics Reveals Hypofunctional Signaling of the nmrTrkA Intracellular Domain

(A) Overview of the SILAC experiment, performed as a biological duplicate for both receptors. Following the trypsin digestion, samples were enriched for phosphopeptides on TiO_2 columns.

(B) Similar number of phosphopeptides were identified and quantified in both rat and chimeric TrkA samples, but significantly more peptides were upregulated when signaling through rat TrkA than through chimeric TrkA (Fisher's exact test, two-tailed p = 0.0155).

(C and D) Activation of rat TrkA triggers stronger phosphorylation of Erk1/2 key regulatory residues than activation of chimeric TrkA.

(E) Regulatory tyrosine-182 residue of p38-α kinase shows stronger phosphorylation when signaling through rat TrkA, but NGF activation does not change phosphorylation levels of the serine-2 residue.

Data in (C)–(E) are presented as mean values from two experiments.

the distribution of phosphoserine (pSer), phosphothreonine (pThr), and phosphotyrosine (pTyr) sites observed in cells transfected with rat or chimeric TrkA was similar to distributions reported previously with cells stimulated with NGF or epidermal growth factor (EGF) (Emdal et al., 2015; Olsen et al., 2006). We next examined the NGF-upregulated phospho-sites and found that significantly more phosphopeptides were upregulated in NGF-treated cells with rat TrkA (361/2,239 [16.8%]) compared to cells with chimeric TrkA (270/2,007 [13.5%]; Figure 4B).

Analysis of upregulated phospho-site sequence motifs was used to extract over-represented and enriched sequence patterns (Chou and Schwartz, 2011; Schwartz and Gygi, 2005). NGF stimulation was associated with the upregulation of a similar pattern of sequence motifs surrounding pSer residues in cells with rat or chimeric TrkA (Figure S5). However, stimulation of the rat TrkA receptor was associated with a more substantial enrichment of proline-containing motifs compared to chimeric TrkA, which is an indicator of stronger

activation of MAPK/CDK protein families (Amanchy et al., 2007).

An additional quantitative proteomics experiment revealed that there was a stronger activation of specific phosphopeptides from Erk2 (MAPK1, pTyr-187) and Erk1 (MAPK3, pTyr-204) (Critton et al., 2008; Sacco et al., 2009) after stimulation of the cells expressing rat TrkA compared to chimeric TrkA (Figure 4C). In addition, western blotting for phosphorylated Erk in HEK293 cells transfected with rat or chimeric TrkA after NGF stimulation revealed reduced levels of phospho-Erk protein after stimulation of the chimeric receptor (Figure 4D). We could also identify and quantify the changes in phosphopeptides from p38-α (MAPK14), a kinase involved in TRPV1 regulation in sensory neurons (Ji et al., 2002; Raingeaud et al., 1995). We observed a stronger increase in the abundance of p38-α derived-phosphopeptides containing the pTyr182 residue after stimulation of rat TrkA compared to chimeric TrkA (Figure 4E). A phosphoserine residue on the same protein (pSer2) (Olsen et al., 2010) did not
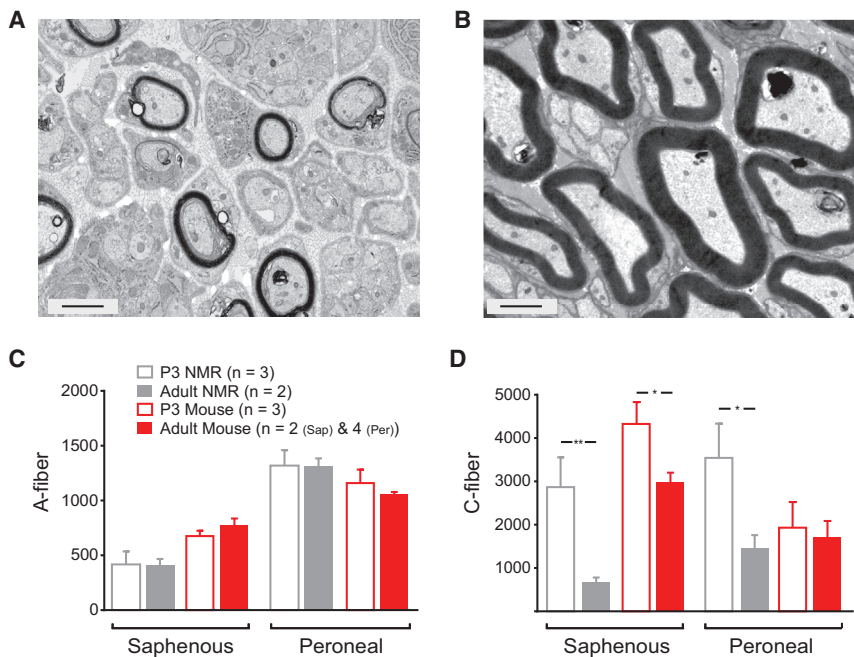
Figure 5. Naked Mole-Rat Pups Have More C-Fibers in Peripheral Nerves than Adults

(A and B) Example electron micrograph of the saphenous nerve of an NMR P3 pup (A) and an adult animal (B). Different myelination stages of single A-fibers and C-fibers within Remak bundles are visible; scale bar, 1 μm.

(C) Numbers of fibers with detectable myelination were comparable for neonatal and adult nerves in both naked mole-rat and mouse.

(D) Quantification of C-fiber number for the saphenous and peroneal nerve in the pup compared to the adult nerve from naked mole-rat and mouse. For comparison, naked mole-rat adult data were taken from St. John Smith et al. (2012) and mouse adult data were taken from Moshourab et al. (2013) and Robertson and Sima (1980) for mouse saphenous and common peroneal nerve, respectively.

Numbers in (C) and (D) indicate the number of animals used for quantification (two nerves per animal). Mann-Whitney *U* test was used (*p < 0.05; **p < 0.01). Data are presented as mean ± SEM.

show any significant change in either condition after NGF stimulation indicating specificity of NGF-mediated activation (Figure 4E).

Developmental Consequences of Hypofunctional TrkA in the Naked Mole-Rat

NGF-TrkA signaling is essential for the survival of embryonic sensory neurons (Lallemend and Ernfors, 2012; Lewin and Barde, 1996). Adult naked mole-rats have a striking paucity of C-fibers in cutaneous nerves (St John Smith et al., 2012), a feature that is reminiscent of NGF/TrkA loss of function in humans and mice (Crowley et al., 1994; Indo et al., 1996). We thus used transmission electron microscopy to quantify the numbers of myelinated and unmyelinated fibers in peripheral nerves of postnatal day 3 (P3) naked mole-rats and mice (Figures 5A and 5B). We compared the numbers of myelinated (or myelinating) axons in the saphenous and common peroneal nerves in neonates with the published values for adult mice and naked mole-rats using identical methods. We found that the number of unmyelinated C-fibers counted in cross-sections from the purely cutaneous saphenous nerve and the mixed common peroneal nerve from naked mole-rats was between 2- and 3.5-fold higher than the number observed in adult nerves (Figure 5D). However, the number of unmyelinated fibers found in the mouse common peroneal nerve did not change between P3 and adult mole-rats, although there was a small attrition of C-fibers from the saphenous nerve (Figure 5D). In contrast, although the peripheral nerves of P3 naked mole-rats and mice are still undergoing myelination (Figures 5A and 5B), the number of fibers with a myelin sheath (A-fibers) was not different between nerves from the neonate and adult (Figure 5C). These data suggested that there is substantial loss of unmyelinated axons from cutaneous and mixed peripheral nerves of naked mole-rats between P3 and adulthood.

DISCUSSION

We dissected the molecular mechanism that underlies the absence of thermal hyperalgesia in the African naked mole-rat (*H. glaber*) (Park et al., 2008). NGF is central player in the generation of thermal hyperalgesia and acts via its receptor TrkA to initiate hyperalgesia in a TRPV1-dependent manner (Bonnington and McNaughton, 2003; Chuang et al., 2001; Lewin et al., 2014). We have shown that lack of heat hyperalgesia in the naked mole-rat is associated with absence of NGF-induced TRPV1 sensitization in sensory neurons. Our data indicate that the key molecular change in the signal transduction pathway from NGF to hyperalgesia is a unique but minimal sequence change in the naked mole-rat TrkA molecule. We provide evidence that between one and three unique amino acid substitutions within the kinase domain make the naked mole-rat TrkA receptor less efficient at engaging downstream signal transduction, including members of the MAPK family of effectors. Efficient NGF signaling is also a prerequisite for the survival and terminal branching of embryonic sensory neurons in the mouse (Crowley et al., 1994; Patel et al., 2000). Interestingly, a hypofunctional TrkA receptor in the naked mole-rat is associated with a striking paucity of unmyelinated C-fibers in adult peripheral nerves (St John Smith et al., 2012). A comparative anatomical study of six other African mole-rat species (for which TrkA sequences were obtained here) indicated that the C-fiber deficit appears to be unique to naked mole-rats (St John Smith et al., 2012). Even though the Mashona mole-rat (*F. darlingi*) shares two out of the three unique amino acid variants found in TrkA kinase domain of the naked mole-rat receptor (Figure S3B), it does not lack C-fibers (St John Smith et al., 2012). We thus postulate that hypofunctional TrkA signaling in vivo may lead to a loss of C-fibers in naked mole-rats. However, newborn naked mole-rats were found to have

many more C-fibers in peripheral nerves than adults. This finding suggests that C-fibers in the naked mole-rat are lost between P3 and adulthood, perhaps as a consequence of hypofunctional TrkA signaling.

Among vertebrate receptors, the TrkA receptor displays the strictest conservation in the intracellular kinase domain (Figure S2). Using chimeric TrkA receptors (rat extracellular/naked mole-rat intracellular), we could show directly that the reduced ability of the naked mole-rat TrkA receptor to sensitize TRPV1 currents is likely localized to the kinase domain (Figure 3). Indeed, biochemical experiments demonstrated a striking reduction in signaling capacity in terms of ligand-dependent tyrosine phosphorylation (Figure S4); however, all the important tyrosine residues in the kinase domain are conserved in the naked mole-rat TrkA molecule (Figure S2). We speculate that insertion of a cysteine for a leucine at position 774 in the naked mole-rat TrkA receptor may alter the efficiency of phosphorylation or recognition of the flanking tyrosine's Tyr751 and Tyr785. Tyrosine 751 has been implicated in binding of the p85 subunit of phosphoinositide 3-kinase (Obermeier et al., 1993b), and Tyr785 serves as a major and selective interaction site for phosphoinositide phospholipase C-γ (Obermeier et al., 1993a). It is of course also possible that accumulated effects of the other variants that are not specific to naked mole-rat TrkA (Figure S3B) contribute to the reduction in receptor signaling we have observed.

Our data strongly suggest that molecular changes in naked mole-rat TrkA molecule alter signal transduction efficiency. Ligand concentration of 100 ng/mL produced almost maximal sensitization of TRPV1 in our oocyte expression system, a similar dose dependence to that found for capsaicin current sensitization in rat sensory neurons (Shu and Mendell, 1999). In contrast, NGF stimulation of chimeric TrkA receptor produced little sensitization of TRPV1 currents at 100 ng/mL but normal sensitization at 1,000 ng/mL (Figure 3C). The maintained efficacy of the naked mole-rat TrkA receptor at very high NGF concentrations is consistent with our previous observation that NGF (500 ng/mL) promotes neurite outgrowth of both mouse and naked mole-rat sensory neurons in culture (Park et al., 2008). However, it is well known that orders-of-magnitude lower concentrations of NGF (<1 ng/mL) are capable of promoting maximal neuronal survival or neurite outgrowth in developing neurons (Davies et al., 1993; Vaillant et al., 2002; Ye et al., 2003). Using a high-resolution quantitative proteomics approach, we found that 10 min after NGF stimulation with 100 ng/mL, there were subtle but significant differences in upregulated phosphopeptides between rat TrkA and a chimeric TrkA containing the naked mole-rat intracellular domain. We obtained evidence of reduced pTyr on peptides belonging to MAPK proteins, including p38α, which has been directly implicated in the sensitization of TRPV1 (Ji et al., 2002).

Surprisingly, naked mole-rat pups do not show the deficit in C-fibers that we had observed in adult animals (Figure 5). It thus appears that the signaling capacity of the naked mole-rat TrkA is sufficient to support the survival and functional development of sensory neurons during embryonic development (Crowley et al., 1994; Lechner et al., 2009). NGF is functionally important for the maintenance of mature sensory neurons (Lewin et al., 2014), but rodents exposed to NGF-function blocking antibodies exhibit death of sympathetic neurons, but probably not sensory neurons (Gorin and Johnson, 1980; Lewin et al., 1992; Ruberti et al., 2000). The concentrations of NGF that robustly sensitize TRPV1 in adult neurons are clearly much higher than those needed to support embryonic survival (see above). It is thus conceivable that the molecular changes in the naked mole-rat TrkA receptor that we describe are more relevant to physiological processes that follow strong receptor stimulation. In this context it is interesting to note that NGF signaling in adult naked mole-rat is still capable of producing mechanical hyperalgesia, a process that does not involve TRPV1 (Lewin et al., 2014). It is possible that hypofunctional TrkA signaling leads to the loss of sensory neurons in naked mole-rats after birth. Naked mole-rats have an extraordinarily long gestation period of ~70 days and can live for up to 32 years (Jarvis, 1991; Sanchez et al., 2015). It is thus feasible that developmental events that occur just after birth, like the loss of TrkA expression in approximately half of the nociceptors (Bennett et al., 1998; Molliver et al., 1997), occur over a more protracted period in the naked mole-rat. In this context, it is important to note that some nociceptors in rats and mice are still dependent on NGF for survival for a few days after birth (Crowley et al., 1994; Lewin et al., 1992). We find that the paucity of C-fibers in cutaneous nerves is correlated with molecular changes in the TrkA receptor associated with reduced signaling (Figure S4). However, it is still possible that effects of other as-yet-unknown gene variants in the naked mole-rat potentiate the effects of the TrkA variants to promote postnatal nociceptor loss.

In summary, we provide evidence that evolution has selected for a single-molecule change in the naked mole-rat NGF receptor TrkA that is sufficient to abolish heat hyperalgesia in this species. Mutations in the *trkA* gene are highly detrimental in humans, but here we show that evolution has selected for sequence change(s) in the naked mole-rat gene that are not only functionally powerful but also compatible with species survival and continued fitness. We speculate that heat hyperalgesia is not an essential phenotypic attribute for the naked mole-rat that is adapted to a subterranean habitat in equatorial East Africa, where temperatures have remained constant for millions of years. Other African mole-rat species have apparently not dispensed with efficient TrkA signaling, and we speculate that one reason for this is that the naked mole-rat is probably the most energetically challenged species in this family (Bennett and Faulkes, 2000). Thus, naked mole-rats can make do with a stripped-down nociceptive system, equipped with fewer C-fibers, that requires less energy but is sufficient for acute nociception and mechanical hyperalgesia following injury (Park et al., 2008). Our study illustrates how evolution can select for mechanistically novel single-molecule changes that exert dramatic phenotypic effects but are compatible with the maintenance of species fitness.

EXPERIMENTAL PROCEDURES

DRG Neuron and Cell Culture

Animal housing, care, and protocols for euthanasia were approved by German federal authorities (State of Berlin). Dorsal root ganglia (DRG) neurons were

prepared from both naked mole-rat and mouse as described previously (Park et al., 2008) and plated onto glass coverslips plated with poly-L-lysine (PLL; 200 mg/mL) and laminin (20 μg/mL). CHO and naked mole-rat fibroblast cells were cultured in F12-Ham medium (Life Technologies) and incubated at 37°C in 5% CO_2. For electrophysiology experiments, cells were plated onto PLL-coated plastic dishes and the following day transfected with Lipofectamine (Invitrogen).

Electrophysiology

Recordings from DRG neurons took place after a 10- to 20-min incubation with either IB4-Alexa 488 or IB4-Alexa Fluor 568 (Invitrogen). Whole-cell recordings were made using pipettes (3–6 MΩ resistance) pulled with a Flaming-Brown puller (Sutter Instruments). Extracellular solution contained 140 mM NaCl, 1 mM $MgCl_2$, 2 mM $CaCl_2$, 4 mM KCl, 4 mM glucose, and 10 mM HEPES (pH 7.4) with NaOH. Electrodes were filled with 110 mM KCl, 10 mM NaCl, 1 mM $MgCl_2$, 1 mM EGTA, and 10 mM HEPES (pH 7.3). Solutions were applied and heated using a gravity-driven multi-barrel perfusion system (WAS-02) (Dittert et al., 2006).

X. laevis defoliculated oocytes (stage V or VI) were purchased from EcoCyte Bioscience. Each oocyte was injected in Barth solution using the Nanoject II Auto-Nanoliter Injector (Drummond) with 32.2 nL cRNA mix. Two-electrode voltage-clamp recordings were performed at room temperature 3–5 days after injection using a GeneClamp500B Amplifier, Digidata 1322A, and pClamp 8.0 Software (Axon Instruments). Additional details are available in Supplemental Experimental Procedures.

Molecular Biology and RNA Sequencing

Cloning of naked mole-rat Trpv1 was described before (Smith et al., 2011). In order to clone naked mole-rat TrkA, total RNA was isolated from DRGs with TRIzol (Life Technologies) and dissolved in 30 μL RNase-free water. 1–3 μg total RNA and oligo(dT) and random hexamers (BioTeZ) were used for cDNA synthesis using SuperScript III Reverse Transcriptase (Life Technologies).

To sequence the coding DNA sequence (CDS) for the TrkA intracellular kinase domain of other African mole-rat species, primers specific for NMR TrkA were used to amplify exons 12–17 from species' genomic DNA. Five mole-rats representative of the Bathyergidae family were used: Giant (*F. mechowii*), Damaraland (*Fukomys damarensis*), Mashona (*Fukomys darlingi*), Natal (*Cryptomys hottentotus natalensis*), and Emin's (*Heliophobius emini*) mole-rats. RNA-seq data for *F. darlingi* were generated from three brain samples using paired-end, strand-specific (dUTP) libraries that were sequenced on an Illumina HiSeq2000 platform. The accession number for the annotated transcriptome and the sequencing reads from the Mashona mole-rat reported in this paper is NCBI: PRJNA303968. Additional details are available in Supplemental Experimental Procedures.

Immunocytochemistry and Calcium Imaging

Standard immunohistochemistry and immunocytochemistry protocols on NMR and mouse DRGs were used using an anti-TrkA antibody (kind gift from L.F. Reichardt, UCSF) and IB4-488. Immunofluorescent images were examined with a Leica DM 5000B microscope and MetaVue software (Visitron).

Calcium imaging was conducted as described previously (Milenkovic et al., 2007). Standard Fura-2 ratiometric calcium imaging was conducted to measure responses to capsaicin in CHO and naked mole-rat fibroblast cells transfected with rat TRPV1and NMR TRPV1, respectively, with or without rTrkA. An inverted microscope (Zeiss Observer A1) equipped with the MetaFluor photonics imaging system, including Polychromator V or DG4 (Sutter Instruments), and a CoolSNAP ES camera (Visitron) was used for cell imaging. Additional details are available in Supplemental Experimental Procedures.

MS-Based Protein Quantification Using SILAC

SILAC-labeled HEK293 cells were transfected with TrkA constructs (rat or chimeric) and pEGFP plasmid (5:1) with polyethylenimine. 24 hr after transfection, cells were serum starved and stimulated for 10 min with 100 ng/mL NGF (murine 2.5S, Promega) or left untreated. Equal amounts of protein from each SILAC pair were mixed together. Protein mixtures were reduced with DTT, al-

kylated with iodoacetamide, pre-digested with Lysyl endopeptidase (LysC, Wako), and subjected to trypsin digestion overnight. Peptides were purified from stop-and-go extraction (STAGE) tips. Phosphopeptide enrichment was performed on 0.5 mg TiO_2 beads. Phosphopeptides were separated on a monolithic column (100 μm inner diameter × 2,000 mm, MonoCap C18 High Resolution 2000 [GL Sciences]; kindly provided by Dr. Yasushi Ishihama [Kyoto University]). The Q Exactive instrument (Thermo Fisher Scientific) was operated in the data-dependent mode, and MaxQuant software was used to identify and quantify proteins. MS/MS spectra were searched using the Andromeda search engine. Additional details are available in Supplemental Experimental Procedures.

ACCESSION NUMBERS

The accession number for the annotated transcriptome and the sequencing reads from the Mashona mole-rat reported in this paper is NCBI: PRJNA303968.

SUPPLEMENTAL INFORMATION

Supplemental Information includes Supplemental Experimental Procedures, five figures, and one table and can be found with this article online at http://dx.doi.org/10.1016/j.celrep.2016.09.035.

AUTHOR CONTRIBUTIONS

ACKNOWLEDGMENTS

REFERENCES

Amanchy, R., Periaswamy, B., Mathivanan, S., Reddy, R., Tattikota, S.G., and Pandey, A. (2007). A curated compendium of phosphorylation motifs. Nat. Biotechnol. 25, 285–286.

Averill, S., McMahon, S.B., Clary, D.O., Reichardt, L.F., and Priestley, J.V. (1995). Immunocytochemical localization of trkA receptors in chemically identified subgroups of adult rat sensory neurons. Eur. J. Neurosci. 7, 1484–1494.

Bennett, N.C., and Faulkes, C.G. (2000). African Mole-Rats: Ecology and Eusociality (Cambridge University Press).

Bennett, D.L., Michael, G.J., Ramachandran, N., Munson, J.B., Averill, S., Yan, Q., McMahon, S.B., and Priestley, J.V. (1998). A distinct subgroup of small DRG cells express GDNF receptor components and GDNF is protective for these neurons after nerve injury. J. Neurosci. 18, 3059–3072.

Bhave, G., Hu, H.-J., Glauner, K.S., Zhu, W., Wang, H., Brasier, D.J., Oxford, G.S., and Gereau, R.W., 4th. (2003). Protein kinase C phosphorylation sensitizes but does not activate the capsaicin receptor transient receptor potential vanilloid 1 (TRPV1). Proc. Natl. Acad. Sci. USA *100*, 12480–12485.

Bonnington, J.K., and McNaughton, P.A. (2003). Signalling pathways involved in the sensitisation of mouse nociceptive neurones by nerve growth factor. J. Physiol. *551*, 433–446.

Carvalho, O.P., Thornton, G.K., Hertecant, J., Houlden, H., Nicholas, A.K., Cox, J.J., Rielly, M., Al-Gazali, L., and Woods, C.G. (2011). A novel NGF mutation clarifies the molecular mechanism and extends the phenotypic spectrum of the HSAN5 neuropathy. J. Med. Genet. *48*, 131–135.

Caterina, M.J., Leffler, A., Malmberg, A.B., Martin, W.J., Trafton, J., Petersen-Zeitz, K.R., Koltzenburg, M., Basbaum, A.I., and Julius, D. (2000). Impaired nociception and pain sensation in mice lacking the capsaicin receptor. Science *288*, 306–313.

Chou, M.F., and Schwartz, D. (2011). Biological sequence motif discovery using motif-x. Curr. Protoc. Bioinformatics *Chapter 13*, Unit 13.15–24.

Chuang, H.H., Prescott, E.D., Kong, H., Shields, S., Jordt, S.E., Basbaum, A.I., Chao, M.V., and Julius, D. (2001). Bradykinin and nerve growth factor release the capsaicin receptor from PtdIns(4,5)P2-mediated inhibition. Nature *411*, 957–962.

Clary, D.O., Weskamp, G., Austin, L.R., and Reichardt, L.F. (1994). TrkA cross-linking mimics neuronal responses to nerve growth factor. Mol. Biol. Cell *5*, 549–563.

Critton, D.A., Tortajada, A., Stetson, G., Peti, W., and Page, R. (2008). Structural basis of substrate recognition by hematopoietic tyrosine phosphatase. Biochemistry *47*, 13336–13345.

Crowley, C., Spencer, S.D., Nishimura, M.C., Chen, K.S., Pitts-Meek, S., Armanini, M.P., Ling, L.H., McMahon, S.B., Shelton, D.L., Levinson, A.D., et al. (1994). Mice lacking nerve growth factor display perinatal loss of sensory and sympathetic neurons yet develop basal forebrain cholinergic neurons. Cell *76*, 1001–1011.

Davies, A.M., Lee, K.F., and Jaenisch, R. (1993). p75-deficient trigeminal sensory neurons have an altered response to NGF but not to other neurotrophins. Neuron *11*, 565–574.

Davies, K.T.J., Bennett, N.C., Tsagkogeorga, G., Rossiter, S.J., and Faulkes, C.G. (2015). Family Wide Molecular Adaptations to Underground Life in African Mole-Rats Revealed by Phylogenomic Analysis. Mol. Biol. Evol. *32*, 3089–3107. http://dx.doi.org/10.1093/molbev/msv175.

Dittert, I., Benedikt, J., Vyklický, L., Zimmermann, K., Reeh, P.W., and Vlachová, V. (2006). Improved superfusion technique for rapid cooling or heating of cultured cells under patch-clamp conditions. J. Neurosci. Methods *151*, 178–185.

Dyck, P.J., Peroutka, S., Rask, C., Burton, E., Baker, M.K., Lehman, K.A., Gillen, D.A., Hokanson, J.L., and O'Brien, P.C. (1997). Intradermal recombinant human nerve growth factor induces pressure allodynia and lowered heat-pain threshold in humans. Neurology *48*, 501–505.

Einarsdottir, E., Carlsson, A., Minde, J., Toolanen, G., Svensson, O., Solders, G., Holmgren, G., Holmberg, D., and Holmberg, M. (2004). A mutation in the nerve growth factor beta gene (NGFB) causes loss of pain perception. Hum. Mol. Genet. *13*, 799–805.

Emdal, K.B., Pedersen, A.-K., Bekker-Jensen, D.B., Tsafou, K.P., Horn, H., Lindner, S., Schulte, J.H., Eggert, A., Jensen, L.J., Francavilla, C., and Olsen, J.V. (2015). Temporal proteomics of NGF-TrkA signaling identifies an inhibitory role for the E3 ligase Cbl-b in neuroblastoma cell differentiation. Sci. Signal. *8*, ra40.

Gorin, P.D., and Johnson, E.M.J., Jr. (1980). Effects of exposure to nerve growth factor antibodies on the developing nervous system of the rat: an experimental autoimmune approach. Dev. Biol. *80*, 313–323.

Hanack, C., Moroni, M., Lima, W.C., Wende, H., Kirchner, M., Adelfinger, L., Schrenk-Siemens, K., Tappe-Theodor, A., Wetzel, C., Kuich, P.H., et al. (2015). GABA blocks pathological but not acute TRPV1 pain signals. Cell *160*, 759–770.

Hempstead, B.L., Rabin, S.J., Kaplan, L., Reid, S., Parada, L.F., and Kaplan, D.R. (1992). Overexpression of the trk tyrosine kinase rapidly accelerates nerve growth factor-induced differentiation. Neuron *9*, 883–896.

Indo, Y., Tsuruta, M., Hayashida, Y., Karim, M.A., Ohta, K., Kawano, T., Mitsubuchi, H., Tonoki, H., Awaya, Y., and Matsuda, I. (1996). Mutations in the TRKA/NGF receptor gene in patients with congenital insensitivity to pain with anhidrosis. Nat. Genet. *13*, 485–488.

Jarvis, J. (1991). Reproduction of naked mole-rats. In The Biology of the Naked Mole-Rat, P.W. Sherman, J.U.M. Jarvis, and R.D. Alexander, eds. (Princeton University Press), pp. 384–425.

Ji, R.-R., Samad, T.A., Jin, S.-X., Schmoll, R., and Woolf, C.J. (2002). p38 MAPK activation by NGF in primary sensory neurons after inflammation increases TRPV1 levels and maintains heat hyperalgesia. Neuron *36*, 57–68.

Kaplan, D.R., Hempstead, B.L., Martin-Zanca, D., Chao, M.V., and Parada, L.F. (1991). The trk proto-oncogene product: a signal transducing receptor for nerve growth factor. Science *252*, 554–558.

Katz, N., Borenstein, D.G., Birbara, C., Bramson, C., Nemeth, M.A., Smith, M.D., and Brown, M.T. (2011). Efficacy and safety of tanezumab in the treatment of chronic low back pain. Pain *152*, 2248–2258.

Keane, M., Craig, T., Alföldi, J., Berlin, A.M., Johnson, J., Seluanov, A., Gorbunova, V., Di Palma, F., Lindblad-Toh, K., Church, G.M., and de Magalhães, J.P. (2014). The Naked Mole Rat Genome Resource: facilitating analyses of cancer and longevity-related adaptations. Bioinformatics *30*, 3558–3560.

Kim, E.B., Fang, X., Fushan, A.A., Huang, Z., Lobanov, A.V., Han, L., Marino, S.M., Sun, X., Turanov, A.A., Yang, P., et al. (2011). Genome sequencing reveals insights into physiology and longevity of the naked mole rat. Nature *479*, 223–227.

Klein, R., Jing, S.Q., Nanduri, V., O'Rourke, E., and Barbacid, M. (1991). The trk proto-oncogene encodes a receptor for nerve growth factor. Cell *65*, 189–197.

Koplas, P.A., Rosenberg, R.L., and Oxford, G.S. (1997). The role of calcium in the desensitization of capsaicin responses in rat dorsal root ganglion neurons. J. Neurosci. *17*, 3525–3537.

Lallemend, F., and Ernfors, P. (2012). Molecular interactions underlying the specification of sensory neurons. Trends Neurosci. *35*, 373–381.

Lane, N.E., Schnitzer, T.J., Birbara, C.A., Mokhtarani, M., Shelton, D.L., Smith, M.D., and Brown, M.T. (2010). Tanezumab for the treatment of pain from osteoarthritis of the knee. N. Engl. J. Med. *363*, 1521–1531.

Lechner, S.G., Frenzel, H., Wang, R., and Lewin, G.R. (2009). Developmental waves of mechanosensitivity acquisition in sensory neuron subtypes during embryonic development. EMBO J. *28*, 1479–1491.

Lewin, G.R., and Barde, Y.A. (1996). Physiology of the neurotrophins. Annu. Rev. Neurosci. *19*, 289–317.

Lewin, G.R., and Mendell, L.M. (1993). Nerve growth factor and nociception. Trends Neurosci. *16*, 353–359.

Lewin, G.R., Ritter, A.M., and Mendell, L.M. (1992). On the role of nerve growth factor in the development of myelinated nociceptors. J. Neurosci. *12*, 1896–1905.

Lewin, G.R., Ritter, A.M., and Mendell, L.M. (1993). Nerve growth factor-induced hyperalgesia in the neonatal and adult rat. J. Neurosci. *13*, 2136–2148.

Lewin, G.R., Rueff, A., and Mendell, L.M. (1994). Peripheral and central mechanisms of NGF-induced hyperalgesia. Eur. J. Neurosci. *6*, 1903–1912.

Lewin, G.R., Lechner, S.G., and Smith, E.S.J. (2014). Nerve growth factor and nociception: from experimental embryology to new analgesic therapy. Handbook Exp. Pharmacol. *220*, 251–282.

Liang, S., Mele, J., Wu, Y., Buffenstein, R., and Hornsby, P.J. (2010). Resistance to experimental tumorigenesis in cells of a long-lived mammal, the naked mole-rat (Heterocephalus glaber). Aging Cell *9*, 626–635.

Lishko, P.V., Procko, E., Jin, X., Phelps, C.B., and Gaudet, R. (2007). The ankyrin repeats of TRPV1 bind multiple ligands and modulate channel sensitivity. Neuron *54*, 905–918.

Milenkovic, N., Frahm, C., Gassmann, M., Griffel, C., Erdmann, B., Birchmeier, C., Lewin, G.R., and Garratt, A.N. (2007). Nociceptive tuning by stem cell factor/c-Kit signaling. Neuron *56*, 893–906.

Molliver, D.C., Wright, D.E., Leitner, M.L., Parsadanian, A.S., Doster, K., Wen, D., Yan, Q., and Snider, W.D. (1997). IB4-binding DRG neurons switch from NGF to GDNF dependence in early postnatal life. Neuron *19*, 849–861.

Moshourab, R.A., Wetzel, C., Martinez-Salgado, C., and Lewin, G.R. (2013). Stomatin-domain protein interactions with acid-sensing ion channels modulate nociceptor mechanosensitivity. J. Physiol. *591*, 5555–5574.

Numazaki, M., Tominaga, T., Toyooka, H., and Tominaga, M. (2002). Direct phosphorylation of capsaicin receptor VR1 by protein kinase Cepsilon and identification of two target serine residues. J. Biol. Chem. *277*, 13375–13378.

O'Connor, T.P., Lee, A., Jarvis, J.U.M., and Buffenstein, R. (2002). Prolonged longevity in naked mole-rats: age-related changes in metabolism, body composition and gastrointestinal function. Comp. Biochem. Physiol. A Mol. Integr. Physiol. *133*, 835–842.

Obermeier, A., Lammers, R., Wiesmüller, K.H., Jung, G., Schlessinger, J., and Ullrich, A. (1993a). Identification of Trk binding sites for SHC and phosphatidylinositol 3′-kinase and formation of a multimeric signaling complex. J. Biol. Chem. *268*, 22963–22966.

Obermeier, A., Halfter, H., Wiesmüller, K.H., Jung, G., Schlessinger, J., and Ullrich, A. (1993b). Tyrosine 785 is a major determinant of Trk—substrate interaction. EMBO J *3*, 933–941.

Olsen, J.V., Blagoev, B., Gnad, F., Macek, B., Kumar, C., Mortensen, P., and Mann, M. (2006). Global, in vivo, and site-specific phosphorylation dynamics in signaling networks. Cell *127*, 635–648.

Olsen, J.V., Vermeulen, M., Santamaria, A., Kumar, C., Miller, M.L., Jensen, L.J., Gnad, F., Cox, J., Jensen, T.S., Nigg, E.A., et al. (2010). Quantitative phosphoproteomics reveals widespread full phosphorylation site occupancy during mitosis. Sci. Signal. *3*, ra3.

Ong, S.-E., Blagoev, B., Kratchmarova, I., Kristensen, D.B., Steen, H., Pandey, A., and Mann, M. (2002). Stable isotope labeling by amino acids in cell culture, SILAC, as a simple and accurate approach to expression proteomics. Mol. Cell. Proteomics *1*, 376–386.

Park, T.J., Lu, Y., Jüttner, R., Smith, E.S.J., Hu, J., Brand, A., Wetzel, C., Milenkovic, N., Erdmann, B., Heppenstall, P.A., et al. (2008). Selective inflammatory pain insensitivity in the African naked mole-rat (Heterocephalus glaber). PLoS Biol. *6*, e13.

Patel, T.D., Jackman, A., Rice, F.L., Kucera, J., and Snider, W.D. (2000). Development of sensory neurons in the absence of NGF/TrkA signaling in vivo. Neuron *25*, 345–357.

Petty, B.G., Cornblath, D.R., Adornato, B.T., Chaudhry, V., Flexner, C., Wachsman, M., Sinicropi, D., Burton, L.E., and Peroutka, S.J. (1994). The effect of systemically administered recombinant human nerve growth factor in healthy human subjects. Ann. Neurol. *36*, 244–246.

Prescott, E.D., and Julius, D. (2003). A modular PIP2 binding site as a determinant of capsaicin receptor sensitivity. Science *300*, 1284–1288.

Price, T.J., and Flores, C.M. (2007). Critical evaluation of the colocalization between calcitonin gene-related peptide, substance P, transient receptor potential vanilloid subfamily type 1 immunoreactivities, and isolectin B4 binding in primary afferent neurons of the rat and mouse. J. Pain *8*, 263–272.

Raingeaud, J., Gupta, S., Rogers, J.S., Dickens, M., Han, J., Ulevitch, R.J., and Davis, R.J. (1995). Pro-inflammatory cytokines and environmental stress cause p38 mitogen-activated protein kinase activation by dual phosphorylation on tyrosine and threonine. J. Biol. Chem. *270*, 7420–7426.

Robertson, D.M., and Sima, A.A. (1980). Diabetic neuropathy in the mutant mouse [C57BL/ks(db/db)]: a morphometric study. Diabetes *29*, 60–67.

Ruberti, F., Capsoni, S., Comparini, A., Di Daniel, E., Franzot, J., Gonfloni, S., Rossi, G., Berardi, N., and Cattaneo, A. (2000). Phenotypic knockout of nerve growth factor in adult transgenic mice reveals severe deficits in basal forebrain cholinergic neurons, cell death in the spleen, and skeletal muscle dystrophy. J. Neurosci. *20*, 2589–2601.

Sacco, F., Tinti, M., Palma, A., Ferrari, E., Nardozza, A.P., Hooft van Huijsduijnen, R., Takahashi, T., Castagnoli, L., Cesareni, G., van Huijsduijnen, R.H., et al. (2009). Tumor suppressor density-enhanced phosphatase-1 (DEP-1) inhibits the RAS pathway by direct dephosphorylation of ERK1/2 kinases. J Biol Chem. *284*, 22048–22058.

Sanchez, J.R., Milton, S.L., Corbit, K.C., and Buffenstein, R. (2015). Multifactorial processes to slowing the biological clock: Insights from a comparative approach. Exp. Gerontol. *71*, 27–37.

Schuhmacher, L.N., Husson, Z., and Smith, E.S. (2015). The naked mole-rat as an animal model in biomedical research: current perspectives. Open Access Anim. Physiol. *7*, 137.

Schwartz, D., and Gygi, S.P. (2005). An iterative statistical approach to the identification of protein phosphorylation motifs from large-scale data sets. Nat. Biotechnol. *23*, 1391–1398.

Segal, R.A., and Greenberg, M.E. (1996). Intracellular signaling pathways activated by neurotrophic factors. Annu. Rev. Neurosci. *19*, 463–489.

Segal, R.A., Bhattacharyya, A., Rua, L.A., Alberta, J.A., Stephens, R.M., Kaplan, D.R., and Stiles, C.D. (1996). Differential utilization of Trk autophosphorylation sites. J. Biol. Chem. *271*, 20175–20181.

Shu, X., and Mendell, L.M. (1999). Nerve growth factor acutely sensitizes the response of adult rat sensory neurons to capsaicin. Neurosci. Lett. *274*, 159–162.

Shu, X., and Mendell, L.M. (2001). Acute sensitization by NGF of the response of small-diameter sensory neurons to capsaicin. J. Neurophysiol. *86*, 2931–2938.

Smith, E.S.J., and Lewin, G.R. (2009). Nociceptors: a phylogenetic view. J. Comp. Physiol. A Neuroethol. Sens. Neural Behav. Physiol. *195*, 1089–1106.

Smith, E.S.J., Omerbašić, D., Lechner, S.G., Anirudhan, G., Lapatsina, L., and Lewin, G.R. (2011). The molecular basis of acid insensitivity in the African naked mole-rat. Science *334*, 1557–1560.

St John Smith, E., Purfürst, B., Grigoryan, T., Park, T.J., Bennett, N.C., and Lewin, G.R. (2012). Specific paucity of unmyelinated C-fibers in cutaneous peripheral nerves of the African naked-mole rat: comparative analysis using six species of Bathyergidae. J. Comp. Neurol. *520*, 2785–2803.

Vaillant, A.R., Zanassi, P., Walsh, G.S., Aumont, A., Alonso, A., and Miller, F.D. (2002). Signaling mechanisms underlying reversible, activity-dependent dendrite formation. Neuron *34*, 985–998.

Woolf, C.J., Safieh-Garabedian, B., Ma, Q.-P., Crilly, P., and Winter, J. (1994). Nerve growth factor contributes to the generation of inflammatory sensory hypersensitivity. Neuroscience *62*, 327–331.

Ye, H., Kuruvilla, R., Zweifel, L.S., and Ginty, D.D. (2003). Evidence in support of signaling endosome-based retrograde survival of sympathetic neurons. Neuron *39*, 57–68.

Zhang, X., Huang, J., and McNaughton, P.A. (2005). NGF rapidly increases membrane expression of TRPV1 heat-gated ion channels. EMBO J. *24*, 4211–4223.

Supplemental Information

Hypofunctional TrkA Accounts for the Absence of

Pain Sensitization in the African Naked Mole-Rat

Damir Omerbašić, Ewan St. J. Smith, Mirko Moroni, Johanna Homfeld, Ole Eigenbrod, Nigel C. Bennett, Jane Reznick, Chris G. Faulkes, Matthias Selbach, and Gary R. Lewin
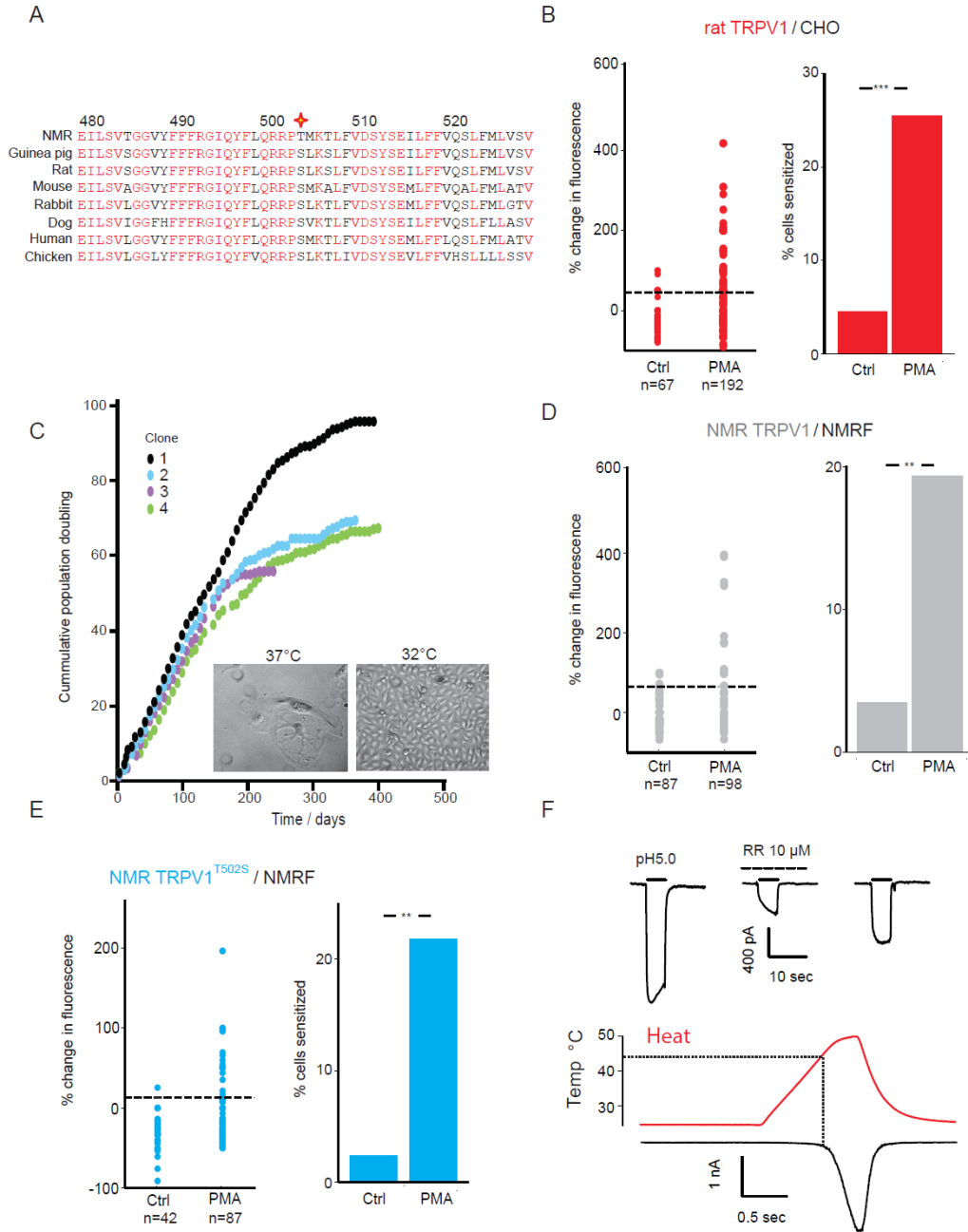
Figure S1 related to Figure 2. Thr502 does not affect PKCε-mediated sensitization of NMR TRPV1. (A) In NMR TRPV1, a conserved serine is substituted by threonine at position 502 (numbering for rat TRPV1). (B) Rat TRPV1 expressed in CHO cells is potentiated by a 30 second pulse of PMA. (C) Generation of naked mole-rat immortalized fibroblasts, four clones were isolated and population doubling (PD) measured weekly. Clone 3 ceased to grow at a cumulative PD of 56, clones 1, 2 and 4 reached PDs of 87, 64 and 60 respectively. Note primary fibroblasts grow normally at 32°C, but form multi-nucleated syncytium at 37°C (D). Naked mole-rat TRPV1 expressed in NMRF cells (clone 1) is similarly potentiated by PMA as rat TRPV1. (E) Naked mole-rat TRPV1T502S expressed in NMRF cells is potentiated by PMA. Chi-squared test; **p < 0.01, ***p < 0.001. (F) pH5.0 solution elicits inward currents in *Trpv1*$^{-/-}$ mouse neurons transfected with naked mole-rat *Trpv1*, currents were inhibited by 10 μM ruthenium red (RR) and transfected *Trpv1*$^{-/-}$ DRG neurons displayed heat-activated currents with mean thresholds of 44.4 ± 0.7°C (n = 5), example heat activated current shown is from a *Trpv1*$^{-/-}$ DRG neuron transfected with naked mole-rat *Trpv1*.
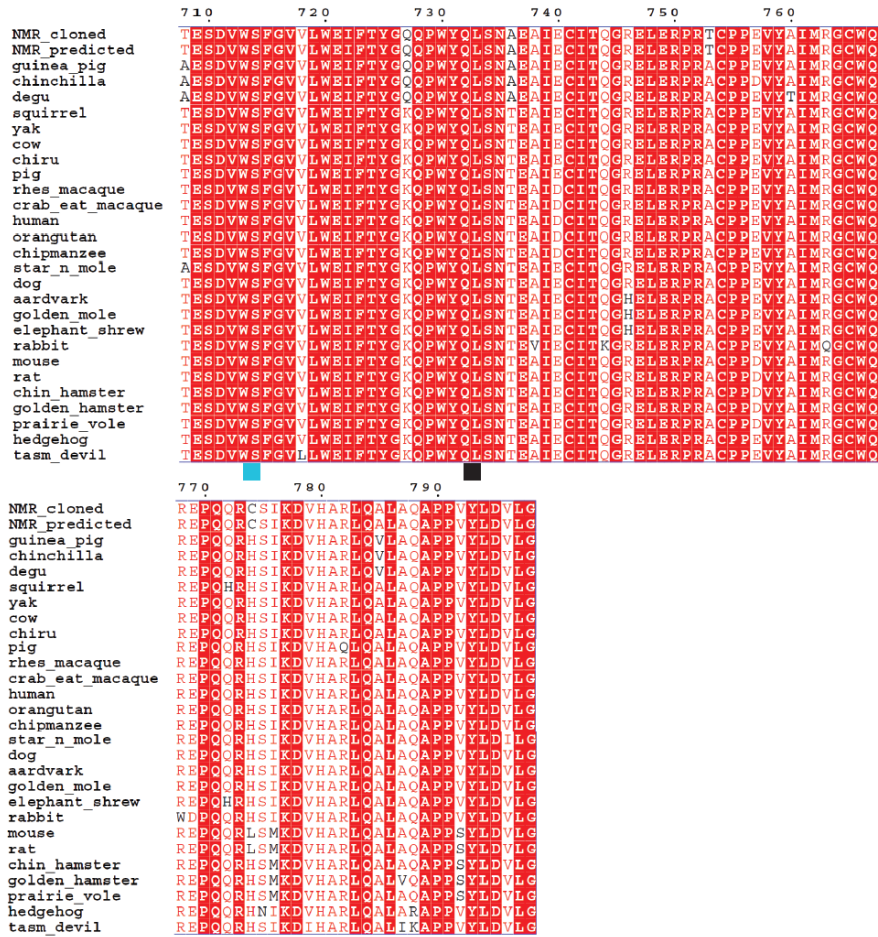
Figure S2 related to Figure 3. Sequence alignment of naked mole-rat TrkA peptide sequence. Cloned and predicted naked mole-rat TrkA sequences (Kim et al., 2011) were aligned with sequences available from public databases. (A) Domain 5 of the extracellular region responsible for NGF binding shows less sequence conservation than the intracellular kinase domain (B). Black squares represent conserved naked mole-rat tyrosines; Tyr759 (human Tyr751) and Tyr793 (human Tyr785). Turquoise square indicates a residue solely found in the naked mole-rat TrkA sequence (see also Figure S3A).
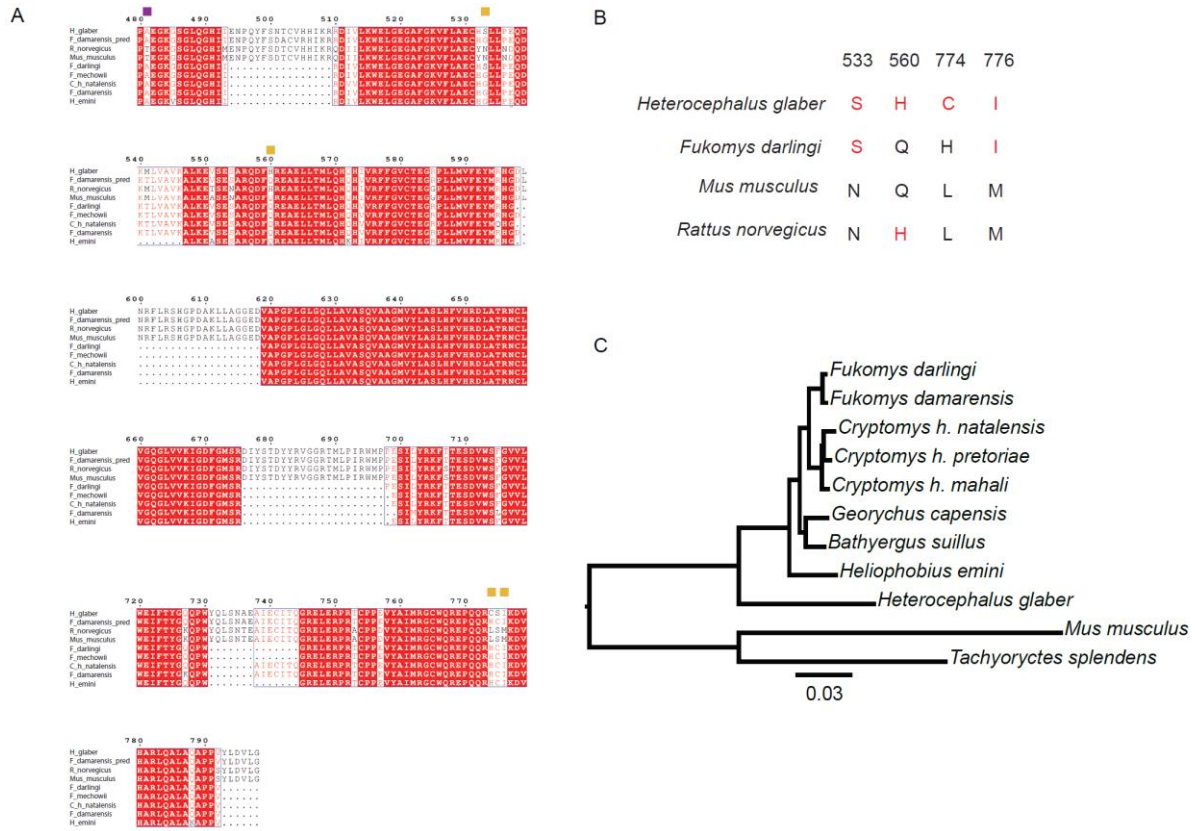
Figure S3 related to Figure 3. Comparison of naked mole-rat TrkA kinase domain sequences those of five other African mole-rat species. (A) Alignment of the TrkA kinase domain sequence for mouse (*M. musculus*), naked mole-rat (*H. glaber*), Giant (*Fukomys mechowii*), Mashona (*F. darlingi*), Natal (*Cryptomys hottentotus natalensis*), Damaraland (*F. damarensis*), and Emin's mole-rat (*Heliophobius emini*)(Faulkes et al., 2011). A purple square represents a bathyergid-specific amino acid variant while orange squares represent the residues defining unique naked mole-rat TrkA kinase domain sequence. (B) Unusual residues that are shared between the naked mole-rat and the designated species are highlighted in red. Numbering is based on NMR TrkA. (C) Phylogenetic relationships between African mole-rat species were calculated from 827 transcripts per species with *Mus musculus* and *Tachyoryctes splendens* (Tanzanian root rat) as outgroups. Sequences were aligned using Clustal Omega (version 1.2.0). A phylogenetic tree was calculated with a maximum likelihood approach implemented in the RAxML tool (version 8.2.3). The *F. darlingi* sequences were obtained from our RNAseq data after de novo transcriptome assembly, publicly available RNAseq data was used to assemble sequences from the other African mole-rat species (see Table S1 for details*).* Branch lengths are proportional to the average number of substitutions per site.
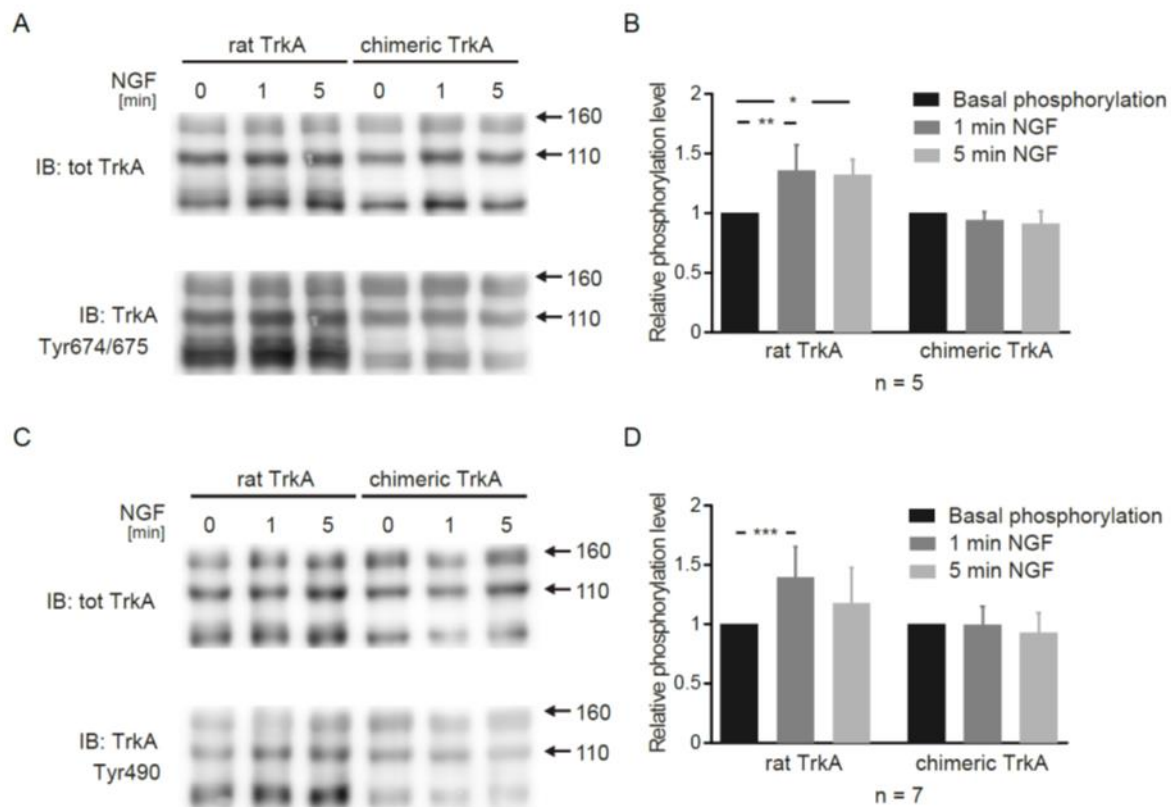
Figure S4 related to Figure 3. NGF-induced activation of rat and chimeric TrkA. Serum-depleted HEK 293 cells expressing either rat or chimeric TrkA were stimulated with NGF (50 or 100 ng/ml) for 1 and 5 minutes, or left untreated, and total cell lysates were subjected for Western blotting analysis. (A) Representative immunoblots against total TrkA and TrkA Tyr674/675. Due to overexpression, a substantial amount of total TrkA was present in its immature form, and only the bands representing mature TrkA (110 and 140 kDa), that can be activated by ligands (Wolf et al., 1998) were used for quantification. (B) Quantification of TrkA intensities from five independent experiments. In rat TrkA, phosphorylation levels were significantly increased after both 1 and 5 minutes of NGF treatment when compared to the basal state. In the cells expressing the chimeric TrkA, the phosphorylation levels after 1 and 5 minute NGF stimulation were not different to the control, non-stimulated receptor. (C) Immunoblotting against total TrkA and TrkA Tyr490. (D) Quantification of TrkA intensities from seven independent experiments. NGF triggered phosphorylation of the Tyr490 residue, where rat TrkA samples showed a significant increase in phosphorylation level after 1 minute NGF stimulation. NGF treatment did not have any effect on the phosphorylation level of the chimeric TrkA Tyr490 residue, where both 1 minute and 5 minute NGF-treated samples were not different to the constitutive phosphorylation level of this receptor. One-sample t-test was used, with the value of basal phosphorylation level set as 1, with *p < 0.05; **p < 0.01 and ***p < 0.001. Data are represented as mean ± SEM.
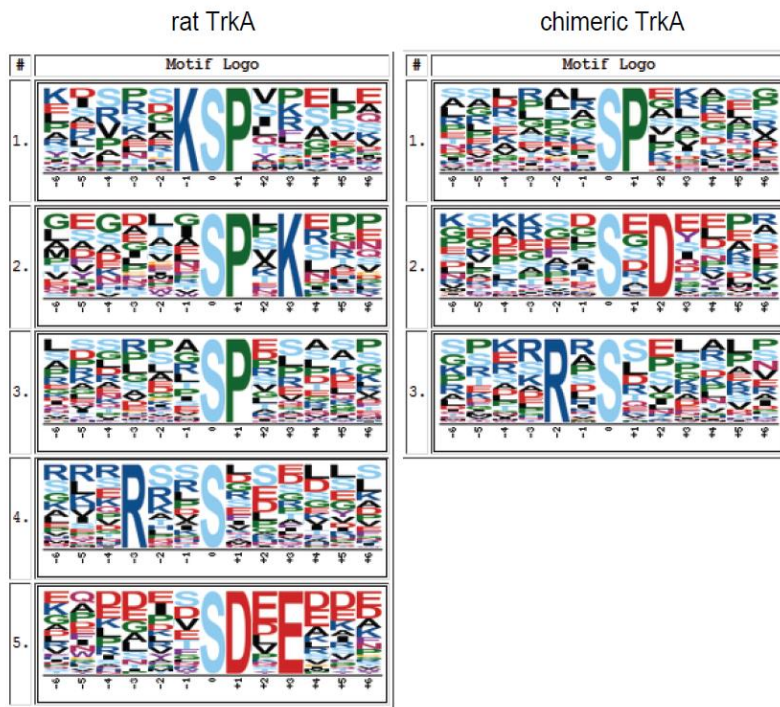
Figure S5 related to Figure 4. Over-represented motifs surrounding upregulated phosphoserine sites when signaling through NGF-stimulated cells expressing either rat or chimeric TrkA. Proline moieties in sequence motifs are common in Erk 1/2 kinase substrate motifs. (Amanchy et al., 2007).

Table S1

Species	SRA accession	# read pairs	# full-length transcripts	% TrkA sequence identified
Fukomys darlingi	SRP066607*	107,855,116	9,798	68
Tachyoryctes splendens	SRR2141217	18,135,605	7,466	35
Heliophobius emini	SRR2141215	17,410,109	1,580	0
Bathyergus suillus	SRR2141210	18,175,296	5,849	26
Georychus capensis	SRR2141216	20,038,942	3,375	0
Cryptomys hottentotus mahali	SRR2141211	17,253,040	5,262	0
Cryptomys hottentotus	SRR2141212	17,290,951	4,973	0
Cryptomys hottentotus	SRR2141213	17,833,375	5,883	0
Fukomys damarensis	SRR2141214	18,220,998	6,109	33

Table S1 related to Figure 3. Summary of transcriptome assemblies from African mole-rat RNAseq data.
Asterisk indicates data set deposited at NCBI accession code PRJNA303968.

Supplemental Experimental Procedures

DRG neuron culture and transfection

Animal housing, care and protocols for killing are registered with and approved by the appropriate German federal authorities (State of Berlin). DRG neurons were prepared from both naked mole-rat and mouse as described previously (Hu et al., 2010; Park et al., 2008) and plated onto glass coverslips plated with poly-L-lysine (200 mg/ml) and laminin (20 µg/ml). Neurons were maintained in DMEM (Life Technologies, U.S.A.) containing 10% heat-inactivated horse serum (Biochrom), 20 mM glutamine, 0.8% glucose, 100 U penicillin and 100 mg/ml streptomycin (Life Technologies) and incubated at 37°C in 5% CO_2. For transfection of naked mole-rat *TRPV1/EGFP* into DRG neurons from *Trpv1*$^{-/-}$ mice (Jax Mice, Bar Harbor, Maine), the Amaxa Nucleofector system was used according to the manufacturer's protocol (Amaxa). All recordings were made within 36 hours of isolation. Note NGF was never added to the medium of cultured DRG neurons as this is known to lead to an up-regulation of heat-activated currents in sensory neurons (Stucky and Lewin, 1999).

CHO cell culture and transfection

CHO cells were cultured in F12-Ham medium (Life Technologies) and incubated at 37°C in 5% CO_2. For electrophysiology experiments cells were plated onto PLL coated plastic dishes and the following day transfected with Lipofectamine (Invitrogen). The plasmid of interest was transfected at a 4:1 ratio with *EGFP*. For calcium imaging experiments cells were plated onto PLL coated glass coverslips and transfected with Fugene (Promega). x*TRPV1* and rat *TrkA* (kind gift of P.A. McNaughton, Kings College London) were transfected at a 5:5:1 ratio with *EGFP*.

Electrophysiology

Recordings took place after a 10 – 20 min incubation with either IB4-Alexa Fluor®-488 or IB4-Alexa Fluor®-568 (Invitrogen) to allow IB4-positive and -negative neurons to be discerned from one another. Whole-cell recordings were made from DRG neurons using pipettes (3 – 6 MΩ resistance) pulled with a Flaming-Brown puller (Sutter Instruments, USA). Extracellular solution contained (mM): NaCl 140, $MgCl_2$ 1, $CaCl_2$ 2, KCl 4, glucose 4, HEPES 10, pH7.4 with NaOH. Electrodes were filled with (mM): KCl 110, NaCl 10, $MgCl_2$ 1, EGTA 1 and HEPES 10, pH7.3. Solutions were applied and heated using a gravity driven multi-barrel perfusion system (WAS-02) (Dittert et al., 2006). All recordings were made using an EPC-10 amplifier in combination with Patchmaster© and Fitmaster© software (HEKA). Pipette and membrane capacitance were compensated using the auto function of Patchmaster and series resistance was compensated by ~70% to minimize voltage errors. IB4-positive of GFP-positive cells were observed using a Polychromator V (Visitron) and MetaFluor (Visitron).

Molecular biology and cloning strategies

Cloning of naked mole-rat *Trpv1* was described before (Smith et al., 2011). QuickChange II XL kit (Stratagene) was used to introduce point mutations. A plasmid coding for rat TrkA was a kind gift from P. A. McNaughton, Cambridge, UK. In order to clone NMR *TrkA*, total RNA was isolated from naked mole-rat DRGs with TRIzol (Life Technologies) and dissolved in 30 µl of RNase-free water. 1 – 3 µg of total RNA, and oligo(dT) and random hexamers (BioTeZ, Berlin) were used for cDNA synthesis using SuperScript III Reverse Transcriptase (Life Technologies). Given that no genomic data was available for naked mole-rat at the time when *TrkA* was cloned, cloning primers were designed in silico by aligning the nucleotide sequence of a *TrkA* coding sequence (CDS) from mouse, rat, human, orangutan and cow. Primers were designed from regions of high sequence conservation. This allowed us to clone and sequence a 2092 bp long transcript, aligning to the 3' of the *TrkA* CDS. Sequence was proofread by cloning the respective exons from NMR genomic DNA. The remaining 305 bp, aligning to the 5' end of the transcript, were devised from Kim et al., 2011. The final 2397 bp long transcript was synthesized and cloned into pUC57 by GenScript.

Chimeric *TrkA* was cloned by overlap extension PCR, by using rat and NMR *TrkA* constructs. The overlapping primers used were 5'TM_nmr CAG TGG AGA AGA GAG ACG ACA CGC CT and 3'TM_rat AGG CGT GTC GTC TCT CTT CTC CAC TGG.

In order to sequence the CDS for the *TrkA* intracellular kinase domain of other African mole-rat species, primers specific for NMR *TrkA* were used to amplify exons 12 – 17 from species' genomic DNA. Five mole-rats representative of the Bathyergidae family were used: Giant (*Fukomys mechowii*), Damaraland (*F. damarensis*), Mashona (*F. darlingi*), Natal (*Cryptomys hottentotus natalensis*) and Emin´s (*Heliophobius emini*) mole-rats.

The constructs used for *Xenopus* oocyte recordings (rat *TRPV1*, rat *TrkA*, NMR *TrkA*, chimeric *TrkA*) were subcloned into a modified pCI vector (Promega), linearized with ClaI and cRNA was synthesized by using the mMESSAGE mMACHINE T7 Transcription Kit (Life Technologies) according to the manufacturer's protocol. The quality and integrity of the cRNA constructs was verified by RNA electrophoresis. The constructs used for activation of TrkA in HEK 293 cells (rat *TrkA*, chimeric *TrkA*) were subcloned into pEXPR-IBA105. All

constructs were verified by Sanger sequencing (Source Bioscience). MultAlin software was used for multiple alignment analysis and visualization (Corpet, 1988).

Xenopus laevis oocyte recordings

cRNA was diluted to 0.55 μg/μl (*TRPV1* : *TrkA* = 2.15 : 1) in ultra-pure water. *X. laevis* defoliculated oocytes (stage V or VI) were purchased from EcoCyte Bioscience and delivered in Barth solution complemented with Pen/Strep. Glass capillaries were pulled on DMZ-Universal Puller (Zeitz, Germany) and each oocyte was injected in Barth solution using the Nanoject II Auto-Nanoliter Injector (Drummond, USA) with 32.2 nl of cRNA mix and kept at 16°C in Barth solution complemented with 10% horse serum and 1% Pen/Strep. Two-electrode voltage-clamp recordings were performed at RT 3 – 5 days after injection using a GeneClamp500B Amplifier, Digidata 1322A and pClamp 8.0 Software (Axon Instruments). Borosilicate glass electrodes (0.5 – 1 MΩ) were filled with 3 M KCl. Solutions were gravity fed with a flow rate of ~5 ml/min using a Bath Perfusion System valve controller (ALA-VM8, Ala Scientific Instruments, USA). Membrane potential was clamped to -40 mV and only those oocytes with leak currents < 500 nA were used for analysis. Between every acid pulse, oocytes were allowed to recover for 2 min with constant oocyte Ringer perfusion. For NGF sensitization, two or three acid pulses (pH5.8) were administered before NGF perfusion (1 – 1000 ng/ml for 5 min) followed by two acid pulses. Current responses right before and after NGF application were used for analysis. Currents were analyzed with pCLAMP9 Software (Axon instruments) after digital filtering at1 kHz.

TrkA activation in HEK cells

HEK 293 cells (grown in DMEM (Gibco), 100 U/ml penicillin, 100 μg/ml streptomycin, 4 mM L-glutamine, 10% fetal calf serum (FCS)) were transfected on Day 0 with either rat or chimeric *TrkA* construct with the PEI reagent. In some experiments, to control for equal level of transfection, cells were co-transfected with a plasmid coding for EGFP protein (DNA ratio *TrkA* : *EGFP* = 5 : 1). The GFP signal was visualized on the Day 1, prior to serum depletion. Recombinant human NGF (Sigma, cat. number N1408) was reconstituted in water (1 μg/ml stock) under sterile conditions and stored at -20°C. Prior to NGF stimulation, cells were serum depleted for 2 hours. 30 min prior to NGF stimulation, 0.5 mM sodium orthovanadate (Sigma) was added in order to block the phosphatases. This step was introduced in order to reduce dephosphorylation by phosphatases in stimulated cells, given that pilot experiments showed low relative increase in TrkA phosphorylation upon NGF stimulation. NGF working solutions (50 and 100 ng/ml) were prepared freshly in DMEM. Cells were incubated with NGF for 1 and 5 min to allow for TrkA receptor activation. Cells were washed 2× in ice cold DPBS and collected by scraping in 1× RIPA buffer (New England Biolabs) supplemented with cOmplete, Mini and PhosSTOP (Roche). Cell lysates were homogenized by passing them 10× and 5× through a 20 G and 23 G needle, respectively. Lysates were incubated for 10 min on ice and cell debris was pelleted at 13.000 rpm at 4°C. The supernatant was subjected to Western blotting. Proteins were transferred to a nitrocellulose membrane (pore size 0.2 μm, GE Healthcare). Membranes were blocked under agitation in blocking solution (5% BSA in TBS, 0.1 % Tween20) for 30 min at RT. Primary (anti-TrkA (kind gift from L.F. Reichardt, UCSF), and TrkA and TrkB Antibody Sampler Kit (CST)) and secondary (anti-rabbit and anti-mouse HRP conjugated) antibodies were diluted in 5% BSA in TBST. The chemiluminescent signal was detected by the photo imager device FusionSolo (Vilber Lourmat) using Super Signal West Dura Chemiluminescent Substrate (Thermo Scientific). For quantification purpose, in order to account for loading and transfer errors, each membrane was immunoblotted twice. Phosphorylation status of a specific residue was assayed first, followed by membrane stripping and immunoblotting for the total TrkA. Membranes were stripped by agitation (75 rpm, 55°C, 25 min) in 25 ml prewarmed stripping solution (2% SDS, 0.8% ß-ME, 80 mM Tris HCl pH6.8).

Calcium imaging

Calcium imaging was conducted as described previously (Milenkovic et al., 2007). Standard Fura-2 ratiometric calcium imaging was conducted to measure responses to capsaicin in CHO and NMRF cells transfected with rat TRPV1and NMR TRPV1 respectively, with rTrkA co-transfected in certain experiments. An inverted microscope (Zeiss Observer A1) equipped with MetaFluor photonics imaging system, including Polychromator V or DG4 (Sutter Instruments), a CoolSNAP ES camera (Visitron) was used for cell imaging. Paired images (340 and 380 nm excitation, 510 nm emission) were collected every 1.7 s. Capsaicin (1μM), NGF (100ng/ml) and PMA (1μM) were diluted in the same extracellular buffer as described for electrophysiology experiments previously. A 5 second capsaicin pulse was followed by 10 minutes perfusion with NGF or buffer lacking NGF before a second capsaicin response was applied. After the first capsaicin pulse only cells whose baseline recovered to at least 50% of the initial value before the second capsaicin application were analyzed. A 10 minute perfusion time was chosen because more cells recovered to within this 50% limit. Sensitization was scored if a cell's percentage change was > mean percentage change + 2 s. d. in controls with percentage change calculated as: (100*(peak 2 – peak 1)/peak 1). For experiments with PMA, normal extracellular buffer was superperfused for 9.5 minutes followed by 30 seconds PMA treatment and then capsaicin. DRG neurons plated on a 5 mm

glass coverslip were placed in a recording chamber of 300 μl volume (Harvard Apparatus) and were continuously perfused with extracellular solution at a rate of 2 ml/min. Cells were loaded with Cal-520 (5 μM, AAT Bioquest) for 1 hour at 37 °C in the presence of Pluronic acid 0.02% dissolved in Ringer solution [(mM): 140 NaCl, 5 KCl, 2 CaCl2, 2 MgCl2, 10 HEPES and 10 glucose, adjusted to pH 7.4]. Capsaicin (100 nM, Tocris) was dissolved in extracellular solution from a stock concentration of 10 mM in ethanol. Capsaicin was perfused for 30 s at 5 minutes interval. A solution contained 100mM KCl and 40mM NaCl was applied at the end of each experiment in order to select only viable and neuronal cells.

Statistical analysis
All statistical analyses were performed with GraphPad Prism 5. For electrophysiological analysis and for calcium imaging in DRG neurons, the Mann-Whitney U test was used to detect differences between neurons subjected to NGF and those not. For calcium imaging in CHO and NMRF cells, Fishers exact test was used. For oocyte recordings, One-way ANOVA with Bonferroni's Multiple Comparison Test was used. For Western blotting analysis, one-sample t-test was used, with the basal state phosphorylation of the non-stimulated samples was set to 1. All data are represented as mean ± SEM, unless otherwise stated. $*p < 0.05$; $**p < 0.01$; $***p < 0.001$ and $****p < 0.0001$.

Immunohistochemistry and immunocytochemistry
Standard immunohistochemistry and immunocytochemistry protocols on NMR and mouse DRGs were used (Wetzel et al., 2007) using an anti-TrkA antibody (kind gift from L.F. Reichardt, UCSF) and IB4-488. Immunofluorescent images were examined with a Leica DM 5000B microscope and MetaVue software (Visitron).

Generation of NMRF cell line
Fibroblast isolation and immortalization was conducted along similar lines to that described previously (Silva et al., 1995). Both kidneys were removed from 1 naked mole-rat and washed 3× in DMEM with 100 U penicillin, 100 mg/ml streptomycin. Tissue was chopped into small pieces and the subsequent sludge was shaken at ~37°C for 10 min in 0.05% trypsin (Sigma) in PBS. A 5 ml aliquot was taken and placed in a 50 ml tube with 5 ml DMEM (with 10% FCS, 100 U penicillin and 100 mg/ml streptomycin). 5 ml 0.05% trypsin was added to the original tissue suspension, shaken again for 10 min and 5 ml were taken again. This procedure was repeated for another 40 min. The trypsin/DMEM suspension was then spun down, cells resuspended in 20 ml supplemented DMEM and plated onto two 10 cm dishes. After initially noticing growth problems at 37°C (as has been noted previously (Salmon et al., 2008), cells from further isolation procedures were incubated at 32°C in 5% CO_2 and split when confluent. A pMSPE plasmid encoding SV40LT (kind gift from J. Fuhrmann, MDC) and G418 (800 μg/ml) were used for immortalization. Clones were selected passaged weekly calculating population doubling (PD). The cells frozen and stored in liquid N_2 could be defrosted and grown at the same rate as the same clone still in culture. Furthermore, after successful transformations cells could grow at 37°C with no major change in weekly PD (tested for 4 passages). However, cells used for experiments were incubated at 32°C to maintain the environment preferred by primary fibroblasts. Clone 1 was used in the experiments described here.

Cell culture for SILAC and sample preparation for MS based protein quantification
HEK293 cells were grown and labelled in SILAC media for at least seven population doublings. SILAC media were prepared as described before (Paul et al., 2011). Briefly, DMEM lacking pyruvate, glutamine, arginine and lysine (GIBCO) were supplemented with 10% dialyzed fetal bovine serum (dFBS, Gibco), pyruvate (1x, GIBCO), Glutamax (1x, GIBCO) and L-proline (20 mg/ml, Sigma). "Heavy" (H) SILAC media contained 28 mg/l $^{13}C_6$ $^{15}N_4$ L-arginine (Arg-10) and 49 mg/l $^{13}C_6$ $^{15}N_2$ L-lysine (Lys-8; all labeled amino acids from Sigma Isotec). "Light" (L) SILAC medium was prepared by adding the corresponding non-labeled amino acids (Arg-0 and Lys-0; Sigma). TrkA plasmids were co-transfected with pEGFP plasmid (5:1) to ensure equal transfection, and linear polyethylenimine (Sigma) was used as a carrier. Cells were grown on 10 cm plates to reach 80%-90% confluence on the day of NGF stimulation. Twenty-four hours after transfection cells were washed once in warm DPBS and incubated for four hours in corresponding media lacking dFBS for serum starvation. Cells were stimulated for 10 min with 100 ng/ml NGF (murine 2.5S, Promega) or left untreated, and washed once in ice-cold DPBS before lysis. For total and upregulated phosphopeptide analysis, a biological duplicate was performed where H-labeled cells were stimulated with NGF, and L-labeled cells were left untreated (PMID 27136326). For assessment of MAPK phosphorylation levels a biological duplicate (label swap) was performed where in the forward set-up, H-cells were stimulated with NGF and L-cells left untreated, and in the reverse set-up L-cells were stimulated with NGF and H-cells left untreated. Cells were collected and lysed in 200 μl lysis buffer (8M urea, 100 mM TrisHCl pH8.0 and benzonase (Merck)) and sonicated in ice-cold water for 5 min.

Protein concentration was measured by DC assay (Bio-Rad) and 250 μg of protein from each SILAC pair were mixed together. Protein mixture was reduced with 10 mM DTT in 50 mM ammonium bicarbonate, alkylated in 50 mM ammonium bicarbonate, 55 mM iodacetamide, pre-digested with Lysyl endopeptidase (LysC, Wako, Osaka, Japan), and subjected to trypsin digestion (Promega) overnight. Digestion was stopped by trifluoroacetic acid (TFA). Peptides were purified from stop-and-go extraction (STAGE) tips (Rappsilber et al., 2003) containing C_{18} Empore disks (3M, Minneapolis, USA) pre-loaded with 10 mg of Reprosil-Gold 120 C_{18}, 3 μm beads (Dr Maisch, Germany). Peptides were eluted from the C_{18} material with 400 μl TiO_2 loading buffer (80% acetonitrile (ACN), 6% TFA). Phosphopeptide enrichment was performed on 0.5 mg TiO_2 beads loaded into small stage tip containing a C_8 Empore disk (3M, Minneapolis, USA). The TiO_2 tips were washed once with TiO_2 loading buffer and once with washing buffer (50% ACN, 0.1% TFA). The first elution was performed with 5% NH_4OH and the second elution was performed with 5% piperidine. Enriched phosphopeptides were purified and eluted from the C_{18} Empore disks (Rappsilber et al., 2003).

LC-MS/MS and MS data processing
Phosphopeptides were separated on a monolithic column (100 μm i.d. x 2,000 mm, MonoCap C_{18} High Resolution 2000 [GL Sciences] kindly provided by Dr. Yasushi Ishihama [Kyoto University]) using 6 hour gradient of increasing ACN concentration at a flow rate of 300 nl/min. The Q Exactive instrument (Thermo Fisher Scientific) was operated in the data dependent mode with a full scan in the Orbitrap followed by top 10 MS/MS scans using higher-energy collision dissociation (HCD). MaxQuant software (v1.5.1.2)(Cox and Mann, 2008) was used to identify and quantify proteins. False discovery rate was set to 1% at both peptide and protein level. Carbamidomethylation of cysteine was selected as a fixed modification, and oxidation of methionine, acetylation of the protein N terminus and phosphorylation of serine, threonine and tyrosine (Phospho (STY)) were used as variable modifications. MS/MS spectra were searched using the Andromeda search engine (Cox et al., 2011) against a UniProt human database (release 2014–10) with an additional 248 common contaminants, and a separate search was performed for rat and chimeric TrkA sequences. All protein sequences were also reversed to generate a target-decoy database. Peptides were scored as up-regulated if $\log_2(NGF+/NGF-) > 0.3$ in at least one replicate. UniProt database was used to assess protein phosphorylation sites of serine, threonine and tyrosine.

Electron microscopy and quantification of peripheral nerves
The general procedure followed for quantification of peripheral nerves was described in (St John Smith et al., 2012). Three NMR pups (postnatal day 3) were intracardially perfused and the nerves of interest were dissected from both legs. Three ultra thin sections were taken from at least two nerves, usually three (nerve loss or damage sometimes occurred during either dissection or the embedding procedure), and on each ultra thin section five images (9422.22 × 7233.52 nm) were taken. Myelinated and unmyelinated axons were counted in these areas in iTEM software (Olympus Soft Imaging Solutions, Münster, Germany) and normalized to the whole nerve. For calculating C:A-fiber ratios (C-fiber count/A-fiber count), an average was taken for each ultra thin section per nerve.

RNA sequencing and de novo transcriptome assembly and annotation
RNAseq data for *Fukomys darlingi* were generated from three brain samples using paired-end, strand-specific (dUTP) libraries that were sequenced on an Illumina HiSeq2000 platform. Multiplexed libraries were sequenced for 2x101 cycles. Quality clipping of the raw reads was performed with Trimmomatic 0.32 (Bolger et al., 2014). Adapters were clipped off using 1 seed mismatch, a palindromic score threshold of 30 and a simple clip threshold of 15. Minimum quality for trailing bases was set to 20. Leading 10 bases were clipped off any read due to a sequence bias introduced by random hexamer priming. Read pairs with at least one read shorter than 30 bases after quality clipping were discarded.

The Trinity tool (Grabherr et al., 2011) (version 20140717) and the Bridger software (Chang et al., 2015) (version 2014-12-01) were used with default parameters to assemble the raw transcriptomes from *Fukomys darlingi* and other African mole-rat species (SRA accession: SRP061925). After the primary assembly, both assemblies were combined using CAP3 (Huang and Madan, 1999) and all merged and non-merged sequences were used for downstream analyses. To identify sequencing library contamination and exclude ribosomal RNA and mitochondrial DNA sequences, the assembly was aligned using BLASTn (Altschul and Lipman, 1990) against mouse and human mRNA sequences from RefSeq (Pruitt et al., 2014), sequences of bacterial genomes often found in laboratory samples (Salter et al., 2014) as well as rRNA sequences from mouse, rat and human and mitochondrial sequences from mouse, rat, human and naked mole-rats. All assembled transcripts with a BLAST hit with an e-value <1e-20 against rRNA or bacterial or mitochondrial DNA that covers at least 10% of the transcript were discarded. Transcripts putatively originating from humans or mice were discarded if they

showed an e-value <1e-20 and sequence identity of >99% and the BLAST hit covered at least 70% of the respective transcript.

To identify protein-coding transcripts in the assembly, we performed a reciprocal best hit (RBH) strategy using UniProt consortium 2014) data sets from four organisms. The UniProt data were downloaded on February 2nd, 2015 and included sequence information from human, mouse, rat and guinea pig. Those species were chosen to be able to annotate transcript sequences that are well conserved among the mammalian kingdom. As proteins are annotated on isoform level in the UniProt data base, only the longest isoform per protein was considered for annotation. After removal of putatively contaminating sequences from the assembly, remaining transcript sequences were mapped to the four protein data sets using BLASTx (Altschul and Lipman, 1990). All hits with an e-value <1e-20 in both forward and reverse direction were considered for further analyses. The same stringency level was used for the alignment of protein sequences against the transcript sequences using tBLASTn (Altschul and Lipman, 1990). Transcripts were discarded as putatively chimeric if there was more than one protein with a best hit to the respective transcript (``collapse factor" >1(O'Neil and Emrich, 2013). RBHs were identified per species and a full-length annotation was assigned if the BLASTx hit covered at least 70% of the protein. To integrate information on transcript annotation across species and to increase the specificity level, a transcript was only annotated as being coding for a specific protein if there existed a full-length annotation in at least two of the four species used for transcript annotation. Sequencing data and annotated transcripts from the Mashona mole-rat can be found under the accession number PRJNA303968 at the NCBI database.

Phylogenetic tree reconstruction:

Eight hundred and twenty-seven (827) transcripts were used per species to reconstruct a phylogenetic tree of the African mole-rats with *Mus musculus* and *Tachyoryctes splendens* as outgroups. *De novo* assembled transcriptomes were used for eight African mole-rat species and *Tachyoryctes splendens*, while naked mole-rat and mouse sequences were obtained from the RefSeq data base using the longest transcript isoform as a gene representative. In all species 827 transcripts were found and aligned using Clustal Omega (Sievers et al., 2011) (version 1.2.0). Their intersecting regions were compared to compute the phylogeny to avoid biases due to falsly assembled 3'- or 5'-UTRs. A phylogenetic tree was calculated with a maximum likelihood approach implemented in the RAxML tool (version 8.2.3). The general time reversible (GTR) model (Tavaré, 1986) was used to account for variable base frequencies and symmetrical substitution rates. A gamma distribution was assumed to underlie the rate heterogeneity over the sites. One hundred rapid bootstrap searches were performed in addition to 20 ML searches, the best ML tree was reported.

Supplemental References

Activities at the Universal Protein Resource (UniProt)., 2014. . Nucleic Acids Res. 42, D191–8. doi:10.1093/nar/gkt1140

Altschul, S.F., Lipman, D.J., 1990. Protein database searches for multiple alignments. Proc. Natl. Acad. Sci. U. S. A. 87, 5509–13.

Amanchy, R., Periaswamy, B., Mathivanan, S., Reddy, R., Tattikota, S.G., Pandey, A., 2007. A curated compendium of phosphorylation motifs. Nat. Biotechnol. 25, 285–286. doi:10.1038/nbt0307-285

Bolger, A.M., Lohse, M., Usadel, B., 2014. Trimmomatic: a flexible trimmer for Illumina sequence data. Bioinformatics 30, 2114–2120. doi:10.1093/bioinformatics/btu170

Chang, Z., Li, G., Liu, J., Zhang, Y., Ashby, C., Liu, D., Cramer, C.L., Huang, X., 2015. Bridger: a new framework for de novo transcriptome assembly using RNA-seq data. Genome Biol. 16, 30. doi:10.1186/s13059-015-0596-2

Corpet, F., 1988. Multiple sequence alignment with hierarchical clustering. Nucleic Acids Res. 16, 10881–10890.

Cox, J., Mann, M., 2008. MaxQuant enables high peptide identification rates, individualized p.p.b.-range mass accuracies and proteome-wide protein quantification. Nat. Biotechnol. 26, 1367–1372. doi:10.1038/nbt.1511

Cox, J., Neuhauser, N., Michalski, A., Scheltema, R.A., Olsen, J. V, Mann, M., 2011. Andromeda: a peptide search engine integrated into the MaxQuant environment. J. Proteome Res. 10, 1794–805. doi:10.1021/pr101065j

Dittert, I., Benedikt, J., Vyklický, L., Zimmermann, K., Reeh, P.W., Vlachová, V., 2006. Improved superfusion technique for rapid cooling or heating of cultured cells under patch-clamp conditions. J. Neurosci. Methods 151, 178–185. doi:16/j.jneumeth.2005.07.005

Faulkes, C.G., Bennett, N.C., Cotterill, F.P.D., Stanley, W., Mgode, G.F., Verheyen, E., 2011. Phylogeography and cryptic diversity of the solitary-dwelling silvery mole-rat, genus Heliophobius (family: Bathyergidae). J. Zool. 285, 324–338. doi:10.1111/j.1469-7998.2011.00863.x

Grabherr, M.G., Haas, B.J., Yassour, M., Levin, J.Z., Thompson, D.A., Amit, I., Adiconis, X., Fan, L., Raychowdhury, R., Zeng, Q., Chen, Z., Mauceli, E., Hacohen, N., Gnirke, A., Rhind, N., di Palma, F., Birren, B.W., Nusbaum, C., Lindblad-Toh, K., Friedman, N., Regev, A., 2011. Full-length transcriptome assembly from RNA-Seq data without a reference genome. Nat. Biotechnol. 29, 644–52. doi:10.1038/nbt.1883

Hu, J., Chiang, L.-Y.Y., Koch, M., Lewin, G.R., 2010. Evidence for a protein tether involved in somatic touch. EMBO J. 29, 855–867. doi:10.1038/emboj.2009.398

Huang, X., Madan, A., 1999. CAP3: A DNA sequence assembly program. Genome Res. 9, 868–77.

Kim, E.B., Fang, X., Fushan, A.A., Huang, Z., Lobanov, A. V, Han, L., Marino, S.M., Sun, X., Turanov, A.A., Yang, P., Yim, S.H., Zhao, X., Kasaikina, M. V, Stoletzki, N., Peng, C., Polak, P., Xiong, Z., Kiezun, A., Zhu, Y., Chen, Y., Kryukov, G. V, Zhang, Q., Peshkin, L., Yang, L., Bronson, R.T., Buffenstein, R., Wang, B., Han, C., Li, Q., Chen, L., Zhao, W., Sunyaev, S.R., Park, T.J., Zhang, G., Wang, J., Gladyshev, V.N., 2011. Genome sequencing reveals insights into physiology and longevity of the naked mole rat. Nature 479, 223–7. doi:10.1038/nature10533

Milenkovic, N., Frahm, C., Gassmann, M., Griffel, C., Erdmann, B., Birchmeier, C., Lewin, G.R., Garratt, A.N., 2007. Nociceptive tuning by stem cell factor/c-Kit signaling. Neuron 56, 893–906. doi:10.1016/j.neuron.2007.10.040

O'Neil, S.T., Emrich, S.J., 2013. Assessing De Novo transcriptome assembly metrics for consistency and utility. BMC Genomics 14, 465. doi:10.1186/1471-2164-14-465

Park, T.J., Lu, Y., Jüttner, R., Smith, E.S.J., Hu, J., Brand, A., Wetzel, C., Milenkovic, N., Erdmann, B., Heppenstall, P.A., Laurito, C.E., Wilson, S.P., Lewin, G.R., Juttner, R., Smith, E.S.J., Hu, J., Brand, A., Wetzel, C., Milenkovic, N., Erdmann, B., Heppenstall, P.A., Laurito, C.E., Wilson, S.P., Lewin, G.R., Jüttner, R., Smith, E.S.J., Hu, J., Brand, A., Wetzel, C., Milenkovic, N., Erdmann, B., Heppenstall, P.A., Laurito, C.E., Wilson, S.P., Lewin, G.R., 2008. Selective inflammatory pain insensitivity in the African naked mole-rat (Heterocephalus glaber). PLoS Biol. 6, e13. doi:10.1371/journal.pbio.0060013

Paul, F.E., Hosp, F., Selbach, M., 2011. Analyzing protein-protein interactions by quantitative mass spectrometry. Methods 54, 387–95. doi:10.1016/j.ymeth.2011.03.001

Pruitt, K.D., Brown, G.R., Hiatt, S.M., Thibaud-Nissen, F., Astashyn, A., Ermolaeva, O., Farrell, C.M., Hart, J., Landrum, M.J., McGarvey, K.M., Murphy, M.R., O'Leary, N.A., Pujar, S., Rajput, B., Rangwala, S.H., Riddick, L.D., Shkeda, A., Sun, H., Tamez, P., Tully, R.E., Wallin, C., Webb, D., Weber, J., Wu, W., DiCuccio, M., Kitts, P., Maglott, D.R., Murphy, T.D., Ostell, J.M., 2014. RefSeq: an update on mammalian reference sequences. Nucleic Acids Res. 42, D756–63. doi:10.1093/nar/gkt1114

Rappsilber, J., Ishihama, Y., Mann, M., 2003. Stop and go extraction tips for matrix-assisted laser desorption/ionization, nanoelectrospray, and LC/MS sample pretreatment in proteomics. Anal. Chem. 75, 663–70.

Salmon, A.B., Sadighi Akha, A.A., Buffenstein, R., Miller, R.A., 2008. Fibroblasts from naked mole-rats are resistant to multiple forms of cell injury, but sensitive to peroxide, ultraviolet light, and endoplasmic reticulum stress. J. Gerontol. A. Biol. Sci. Med. Sci. 63, 232–241.

Salter, S.J., Cox, M.J., Turek, E.M., Calus, S.T., Cookson, W.O., Moffatt, M.F., Turner, P., Parkhill, J., Loman,

N.J., Walker, A.W., 2014. Reagent and laboratory contamination can critically impact sequence-based microbiome analyses. BMC Biol. 12, 87. doi:10.1186/s12915-014-0087-z

Sievers, F., Wilm, A., Dineen, D., Gibson, T.J., Karplus, K., Li, W., Lopez, R., McWilliam, H., Remmert, M., Söding, J., Thompson, J.D., Higgins, D.G., 2011. Fast, scalable generation of high-quality protein multiple sequence alignments using Clustal Omega. Mol. Syst. Biol. 7, 539. doi:10.1038/msb.2011.75

Silva, R. De, Zahra, D.G., Duncan, E.L., Reddel, R.R., 1995. Immortalization of human fibroblasts by liposome-mediated transfer of SV40 early region genes. Methods Cell Sci. 17, 75–81. doi:10.1007/BF00986654

St John Smith, E., Purfürst, B., Grigoryan, T., Park, T.J., Bennett, N.C., Lewin, G.R., 2012. Specific paucity of unmyelinated C-fibers in cutaneous peripheral nerves of the African naked-mole rat: comparative analysis using six species of Bathyergidae. J. Comp. Neurol. 520, 2785–803. doi:10.1002/cne.23133

Stucky, C.L., Lewin, G.R., 1999. Isolectin B(4)-positive and -negative nociceptors are functionally distinct. J. Neurosci. Off. J. Soc. Neurosci. 19, 6497–6505.

Tavaré, S., 1986. Some Probabilistic and Statistical Problems in the Analysis of DNA Sequences. Amer Mathematical Society.